Biomechanics and Modeling in Mechanobiology manuscript No.
(will be inserted by the editor)

A K-BKZ Formulation for Soft-Tissue Viscoelasticity

A regularized fractional-derivative kernel with application to the human calcaneal fat pad

Alan D. Freed[1], **Kai Diethelm**[2]

[1] Bio Science and Technology Branch, MS 49-3
NASA's John H. Glenn Research Center at Lewis Field
21000 Brookpark Road
Cleveland, OH 44135, USA.
e-mail: Alan.D.Freed@nasa.gov
And: Department of Biomedical Engineering, ND-20
The Cleveland Clinic Foundation
9500 Euclid Avenue
Cleveland, OH 44195, USA.
e-mail: FreedA@ccf.org

[2] GNS Gessellschaft für Numerische Simulation mbH
Am Gaußberg 2
38114 Braunschweig, Germany.
e-mail: Diethelm@gns-mbh.com
And: Institut Computational Mathematics
Technische Universität Braunschweig
Pockelsstraße 14
38106 Braunschweig, Germany.
e-mail: K.Diethelm@tu-bs.de

Submitted: 26 May 2005 / Revised version: 31st May 2005

Dedicated to Prof. Ronald L. Bagley.

Abstract A viscoelastic model of the K-BKZ (Kaye 1962; Bernstein et al. 1963) type is developed for isotropic biological tissues, and applied to the fat pad of the human heel. To facilitate this pursuit, a class of elastic solids is introduced through a novel strain-energy function whose elements possess strong ellipticity, and therefore lead to stable material models. The standard fractional-order viscoelastic (FOV) solid is used to arrive at the overall elastic/viscoelastic structure of the model, while

Send offprint requests to: Alan D. Freed
Correspondence to: Alan D. Freed

the elastic potential—via the K-BKZ hypothesis—is used to arrive at the tensorial structure of the model. Candidate sets of functions are proposed for the elastic and viscoelastic material functions present in the model, including a regularized fractional derivative that was determined to be the best. The Akaike information criterion (AIC) is advocated for performing multi-model inference, enabling an objective selection of the best material function from within a candidate set.

Key words nonlinear elasticity – viscoelasticity – finite strain – fractional calculus – Mittag-Leffler function – soft tissue – multi-model inference

1 Introduction

The human heel is comprised of skin, a fat pad, the origin of the plantar aponeurosis tendon and the calcaneal bone. Collectively, the soft tissues therein constitute the heel pad. The heel pad is our body's natural shock absorber, dissipating impulses introduced into the body during normal activity, and thereby attenuating the forces that are transmitted up through the body's skeletal structure (Cavanagh et al. 1984).

A certain amount of loading is needed to maintain healthy bone. Bed-rest studies have demonstrated that prolonged inactivity depletes bone density (Shackelford et al. 2004).

NASA has a need to understand how much force is being transferred into the load-bearing bones of the body during exercise so that effective countermeasure protocols can be developed to help avert bone loss in astronauts during long space missions (Lang et al. 2004). Current devices that measure in-shoe forces beneath the heel have recorded forces that exceed twice body weight when an astronaut ran on a treadmill on Earth; whereas, when running on an identical treadmill located within the International Space Station, using the same in-shoe transducers and a harness attached at the waist pushing the astronaut against the treadmill, maximum forces of about one and one-half times body weight were recorded (Cavanagh et al. In press). To determine how much of this force is actually being transmitted to bone will require numerical analysis. To be able to run such an analysis will require material models for the soft-tissue constituents of the heel pad. Here we develop a viscoelastic material model for the human calcaneal fat pad.

Although the fractional calculus[1] has enjoyed wide application in synthetic polymer rheology (see Podlubny 1999, pp. 268–277, for a brief literature review), it has attracted limited attention in the field of biomechanics: Suki et al. (1994) found the pressure/volume response of a whole lung to be aptly characterized by a Newtonian FOV material model with a fractional order of evolution of 0.1;[2] his

[1] Calculus is the study of properties of functions in one or more variables, using derivatives and integrals. Fractional calculus extends the classic study of integer-order derivatives and integrals to include derivatives and integrals of non-integer order, e.g., $\mathrm{d}^{\pi}y/\mathrm{d}x^{\pi}$.

[2] For the Newtonian FOV model, a fractional order of evolution equaling 1 is the limiting case of a viscous Newtonian fluid, while a fractional order of evolution equaling 0 is the limiting case of an elastic Hookean solid.

colleagues, Yuan et al. (1997, 2000), studied lung tissue and found its fractional order of evolution to be about the same, viz., 0.075; while Chen et al. (2004) applied the same model to agarose gels used for culturing tissues, especially cartilage, and found its value to be about 0.03. These are all values close to that of ideal elasticity, where the order of evolution is 0. In a study of charge dynamics in protein molecules, Glöckle and Nonnenmacher (1995) derived a kinetic equation in the form of a fractional-order integral equation (i.e., a Volterra equation of the second kind with an Abel power-law kernel) and found the charge relaxation in myoglobin to be accurately described by a formula where the fractional order of evolution was set at -0.4.[3] In papers by Carew et al. (2003) and Doehring et al. (2004), the response of aortic heart valves to 1D experiments has been shown to be well represented by a quasi-linear[4] Kelvin-Zener FOV solid with the fractional order of evolution being about 0.25.

In this paper, we present a K-BKZ viscoelastic model tailored to the response of the human calcaneal fat pad loaded in compression. The paper begins with a presentation of the kinematic fields needed to construct such a theory. A novel class of nonlinear elastic solids is then presented that has great potential in the modeling of soft tissues. We use the AIC information theoretic (Burnham and Anderson 2002) to select a 'best' model for the heel pad based on the compression data of Miller-Young et al. (2002)—a power-law model was found to be best. A review of 1D FOV restricted to infinitesimal strains follows, which is then transformed into an equivalent Boltzmann integral equation with a memory-function kernel. This formulation is useful in that it permits an extension into 3D by applying the K-BKZ hypothesis to construct a finite-strain theory. This hypothesis employs the elastic strain-energy function (previously selected) to establish the tensorial structure of the viscoelastic model. Like our elastic material class, there are many candidate models that belong to our viscoelastic material class. In addition to the FOV kernel, four other kernel functions are considered as candidate models. The AIC information theoretic was then used once again to select a 'best' model, this time based on the stress-relaxation experiment of Miller-Young et al. (2002). A regularized fractional derivative (RFD), introduced in App. B, was found to be the best viscoelastic kernel.

Appendices are provided that: **A**, describe how to use the AIC information theoretic; **B**, list the candidate viscoelastic kernels; **C**, derive our viscoelastic constitutive formula using convected tensor fields, and establish how such formulæ map into Cartesian space; and **D**, list series expansions that allow finite-strain constitutive formulæ to be recast as infinitesimal-strain constitutive formulæ.

---

[3] Fractional-order integration and differentiation can be defined as a single operator that is continuous over the order parameter; hence, the term differ-integration (Oldham and Spanier 1974). The accepted notation employs a minus sign (e.g., -0.4) when designating the order of integration, and a plus sign (viz., 0.4) when designating the order of differentiation.

[4] A viscoelastic model is said to be 'quasi-linear' if: the linear strain (or forcing function) of classic (linear) viscoelasticity is replaced by a nonlinear strain measure, the kernel (or memory) function depends solely on time (i.e., strain-time separability applies), and only a first-order integral over time appears in the model. K-BKZ models are quasi-linear.

2 Kinematics

Consider a rectangular Cartesian coordinate system with orthonormal base vectors $\boldsymbol{e}_1$, $\boldsymbol{e}_2$ and $\boldsymbol{e}_3$. We focus our attention on a mass point originally located by the set of coordinates $\boldsymbol{X} = (X_1, X_2, X_3)$ assigned at an arbitrary reference time t_0 in this coordinate frame. At current time t, this mass element is located by a different set of coordinates $\boldsymbol{x} = (x_1, x_2, x_3)$ in the same coordinate frame, while at some intermediate time—say s, $t_0 \le s \le t$—it had coordinates $\boldsymbol{\chi} = (\chi_1, \chi_2, \chi_3)$.

It is supposed that the motion of this mass point through space can be described by a one-parameter family (in time) of locations considered to be continuous and sufficiently differentiable to allow the following deformation gradients to be defined

$$F_{ij}(t_0,t) := \frac{\partial x_i}{\partial X_j}, \quad \widehat{F}_{ij}(s,t) := \frac{\partial x_i}{\partial \chi_j}, \quad \widetilde{F}_{ij}(t_0,s) := \frac{\partial \chi_i}{\partial X_j}, \tag{1}$$

where indices i and j have values $1, 2, 3$. Here these formulæ have been written in component form; in tensor notation they are written as

$$\mathbf{F} = F_{ij}\,\boldsymbol{e}_i \otimes \boldsymbol{e}_j, \quad \widehat{\mathbf{F}} = \widehat{F}_{ij}\,\boldsymbol{e}_i \otimes \boldsymbol{e}_j, \quad \widetilde{\mathbf{F}} = \widetilde{F}_{ij}\,\boldsymbol{e}_i \otimes \boldsymbol{e}_j, \tag{2}$$

where $\otimes$ is the vector outer product. These fields satisfy the identity $\mathbf{F} = \widehat{\mathbf{F}}\,\widetilde{\mathbf{F}}$, or equivalently, $F_{ij} = \widehat{F}_{ik}\widetilde{F}_{kj}$ where the repeated k index is summed over in the usual manner. The ability to invert these fields, guaranteed by the conservation of mass, ensures that a given particle cannot occupy two locations at the same instant in time, and that two discrete locations do not associate with a single particle at any given moment in time.

Deformation fields are two-state fields that can be scalar, vector or tensor valued. Hereafter, arguments denoting the state dependence of these fields are omitted for brevity, at least for the most part. Instead, as in Eq. (2), plain-symboled deformation fields are considered to have a state dependence of (t_0, t); hatted deformation fields are considered to have a state dependence of (s, t); and tilded deformation fields are considered to have a state dependence of (t_0, s).

Affiliated with the above deformation gradients are the left- and right-deformation tensors defined by

$$\mathbf{B} := \mathbf{F}\mathbf{F}^{\mathrm{T}} \quad \text{and} \quad \mathbf{C} := \mathbf{F}^{\mathrm{T}}\mathbf{F}, \tag{3}$$

respectively, where '$^{\mathrm{T}}$' implies transpose (viz., $B_{ij} = F_{ik}F_{jk}$ and $C_{ij} = F_{ki}F_{kj}$). By $\widehat{\mathbf{B}}$ we mean $\widehat{\mathbf{F}}\widehat{\mathbf{F}}^{\mathrm{T}}$, etc. The left-deformation tensor $\mathbf{B}$ of Finger (1894) typically appears in Eulerian constructions, while the right-deformation tensor $\mathbf{C}$ of Green (1841) typically appears in Lagrangian constructions.

For model implementation into numerical codes, like finite elements, it is often useful to split the deformation variables into hydrostatic and deviatoric parts. Following Flory (1961), we assign

$$J := \det\mathbf{F}, \quad \overline{\mathbf{F}} := J^{-1/3}\mathbf{F}, \quad \overline{\mathbf{C}} := \overline{\mathbf{F}}^{\mathrm{T}}\overline{\mathbf{F}}, \quad \overline{\mathbf{B}} := \overline{\mathbf{F}}\,\overline{\mathbf{F}}^{\mathrm{T}}, \tag{4}$$

so that $\det\bar{\mathbf{F}} = 1$, and therefore, $\det\bar{\mathbf{C}} = \det\bar{\mathbf{B}} = 1$, where $\det(\cdot)$ denotes the determinant. Likewise, one can define

$$\hat{J} := \det\hat{\mathbf{F}}, \quad \hat{\bar{\mathbf{F}}} := \hat{J}^{-1/3}\hat{\mathbf{F}}, \quad \hat{\bar{\mathbf{C}}} := \hat{\bar{\mathbf{F}}}^{\mathrm{T}}\hat{\bar{\mathbf{F}}}, \quad \hat{\bar{\mathbf{B}}} := \hat{\bar{\mathbf{F}}}\hat{\bar{\mathbf{F}}}^{\mathrm{T}}, \tag{5}$$

and

$$\tilde{J} := \det\tilde{\mathbf{F}}, \quad \tilde{\bar{\mathbf{F}}} := \tilde{J}^{-1/3}\tilde{\mathbf{F}}, \quad \tilde{\bar{\mathbf{C}}} := \tilde{\bar{\mathbf{F}}}^{\mathrm{T}}\tilde{\bar{\mathbf{F}}}, \quad \tilde{\bar{\mathbf{B}}} := \tilde{\bar{\mathbf{F}}}\tilde{\bar{\mathbf{F}}}^{\mathrm{T}}, \tag{6}$$

so that $\det\hat{\bar{\mathbf{F}}} = \det\tilde{\bar{\mathbf{F}}} = 1$. A bar over a tensorial deformation field implies that it is isochoric (preserves volume), while a hat or a tilde on top of that designates the state in which it is isochoric.

3 Elasticity

Before one can construct a viscoelastic model for soft tissues, it is necessary to quantify the highly nonlinear elastic behavior that dominates soft-tissue response. Specifically, what we are after is the mathematical form of the elastic strain-energy function for the material of interest; herein, the human heel pad. Different tissues are typically governed by different strain-energy functions.

The strain-energy density per unit mass, when written for the Lagrangian frame, is given by

$$\mathrm{d}W = \frac{1}{2\varrho_0}\,\mathrm{tr}(\mathbf{S}\,\mathrm{d}\mathbf{C}), \tag{7}$$

where $\mathrm{tr}(\cdot)$ is the trace operator, while $\mathrm{d}W(\boldsymbol{X};t_0,t,\mathrm{d}t)$ represents the work done over a time increment $\mathrm{d}t$ on a material element with mass density $\varrho = \varrho(\boldsymbol{x};t)$, where $\varrho_0 = \varrho(\boldsymbol{X};t_0)$. Work is caused by an imposed displacement acting on the mass element, manifested here as the strain increment $\frac{1}{2}\mathrm{d}\mathbf{C}(\boldsymbol{X};t_0,t,\mathrm{d}t)$. The material responds to this displacement through the creation of forces, thereby producing a state of stress $\mathbf{S}(\boldsymbol{X};t_0,t)$. It follows that $\frac{\varrho_0}{\varrho} = \det\mathbf{F}$ from the conservation of mass.

Elastic states occur at minima in the strain-energy function W. Therefore, an incompressible elastic solid is defined in the Eulerian frame by the constitutive law

$$\mathbf{T} + \wp\,\mathbf{I} = 2\varrho\,\mathbf{F}\,\frac{\partial W(\mathbf{C})}{\partial\mathbf{C}}\,\mathbf{F}^{\mathrm{T}}, \quad \det\mathbf{F} = 1, \tag{8}$$

where the isochoric constraint for incompressibility, $\det\mathbf{F} = 1$, is introduced into the formula through a Lagrange multiplier $\wp$ multiplying the identity tensor $\mathbf{I}$. Soft tissues are comprised primarily of water, whose bulk modulus is 2.2 GPa. Most of these tissues have shear moduli that typically range between a kPa and 10's of MPa. Consequently, the ratio of their bulk to shear moduli usually lies between 100 and 100,000, depending on the tissue, making incompressibility a reasonable assumption to impose for these tissues. An application of the push-forward operator (Holzapfel 2000, pp. 82–84) transforms the Lagrangian form of this law, which one obtains by minimizing Eq. (7), into the Eulerian expression presented in Eq. (8). The second Piola-Kirchhoff stress $\mathbf{S}$ maps into the Cauchy stress $\mathbf{T}(\boldsymbol{x};t)$ according to the well-known formula $\mathbf{T} = \frac{\varrho}{\varrho_0}\mathbf{F}\mathbf{S}\mathbf{F}^{\mathrm{T}}$.

There are two non-trivial invariants needed to describe an isotropic, incompressible, elastic solid (Rivlin 1948); they are:

$$I = \operatorname{tr}\mathbf{C} \equiv \operatorname{tr}\mathbf{B} \quad \& \quad II = \tfrac{1}{2}\Big(\big(\operatorname{tr}\mathbf{C}\big)^2 - \operatorname{tr}\big(\mathbf{C}^2\big)\Big) = \operatorname{tr}\mathbf{C}^{-1} \equiv \operatorname{tr}\mathbf{B}^{-1}. \tag{9}$$

Consequently, the tensorial dependence of $W(\mathbf{C})$ can be replaced by a scalar one of $W(I, II)$. The strain-energy function W will also depend on a number of material constants. The third invariant is a trivial argument, because $III = \det\mathbf{C} = 1$ from the incompressibility assumption. We will reintroduce the third invariant in §5. An application of the Cayley-Hamilton theorem proves the identity $\frac{1}{2}\big((\operatorname{tr}\mathbf{C})^2 - \operatorname{tr}(\mathbf{C}^2)\big) = \operatorname{tr}\mathbf{C}^{-1}$ provided that $\det\mathbf{C} = 1$, which follows from incompressibility.

We are not free to assign any functional form of our choosing to the strain-energy function. Material stability needs to be taken into consideration. This is especially important so as not to inadvertently incite numeric instability into software codes like finite elements. A critical hypothesis needed for well-posedness of such initial value problems is that the equation of motion be hyperbolic or, equivalently, that the corresponding quasi-static constitutive equation be elliptic. In this regard, Renardy (1985) proved a lemma that establishes a sufficient condition for strong ellipticity in a K-BKZ fluid that has relevance in elasticity as-well-as in K-BKZ viscoelasticity whenever both invariants I and II are active.

Lemma 1 *A sufficient condition for strong ellipticity in an incompressible, isotropic, elastic solid is that its strain-energy function be strictly: monotone in I and II, and convex in $\sqrt{I}$ and $\sqrt{II}$.*

The monotonicity part of Renardy's lemma mandates that the gradients of the strain-energy function (taken with respect to I and II) must be positive; that is,

$$\frac{\partial W}{\partial I} > 0 \quad \text{and} \quad \frac{\partial W}{\partial II} > 0. \tag{10}$$

The convexity part of his lemma mandates that the Hessian of the strain-energy function (taken with respect to $\sqrt{I}$ and $\sqrt{II}$) must be positive definite, which via Sylvester's theorem (a.k.a. the criterion of Hurwitz) requires that

$$\frac{\partial^2 W}{\big(\partial\sqrt{I}\big)^2} > 0 \quad \text{and} \quad \frac{\partial^2 W}{\big(\partial\sqrt{I}\big)^2}\,\frac{\partial^2 W}{\big(\partial\sqrt{II}\big)^2} > \left(\frac{\partial^2 W}{\partial\sqrt{I}\,\partial\sqrt{II}}\right)^2. \tag{11}$$

An important example of a strain-energy function that satisfies this lemma is the sum $W \propto I + II$. Simple counterexamples that do not satisfy this lemma include: the product $W \propto I\,II$, which is monotonic but not convex; the ratio $W \propto I/II$, which is neither monotonic nor convex; and the product sum $W \propto I^2 II + I\,II^2$, which is monotonic but not convex in a large region surrounding the stress-free state where $\mathbf{B} = \mathbf{I}$. Many other counterexamples can also be constructed.

Rivlin and Saunders (1951) introduced a phenomenological class of incompressible elastic solids whose strain-energy function is given by

$$2\varrho W_{MR} = \sum_{\alpha=0,\beta=0}^{\infty} C_{\alpha\beta}\,(I-3)^{\alpha}(II-3)^{\beta}, \quad C_{00} = 0, \tag{12}$$

where the $C_{\alpha\beta}$ are material constants to be obtained through parameter estimation procedures. The literature often refers to this as the Mooney-Rivlin solid. The neo-Hookean solid (derived from statistical molecular physics) has a non-zero coefficient for C_{10}, while the phenomenological Mooney solid has non-zero coefficients for C_{10} and C_{01} (Treloar 1975, pp. 212–213). Both are popular models in the rubber elasticity literature. To satisfy Lemma 1, the coefficients in the neo-Hookean and Mooney solids must all be positive valued. Mixed coefficients $C_{\alpha\beta}$, where $\alpha > 0$ and $\beta > 0$, associate with terms that do not satisfy Lemma 1, in general.

We propose an alternative phenomenological class of incompressible elastic solids that satisfies Lemma 1, and which finds application in biological tissues. Elements of this material class have gradients of strain energy that produce formulæ for stress $\mathbf{T}$ that are proportional to *strain* fields (e.g., $\frac{1}{4}(\mathbf{B}-\mathbf{B}^{-1})$ in the simplest case). It is the tensorial strain measure that becomes $\mathbf{0}$ whenever $\mathbf{B}=\mathbf{I}$ in our material class. In contrast, the Mooney-Rivlin class of elastic solids in Eq. (12) produces formulæ for $\mathbf{T}$ that are proportional to the *deformation* fields $\mathbf{B}$ and $-\mathbf{B}^{-1}$, and as such, they rely on the Lagrange multiplier $\wp$ in Eq. (8) to absorb all residual strain occurring at $\mathbf{B}=\mathbf{I}$. This is permissible, mathematically; it is just not desirable, physically, in our opinion.

The Eulerian strain tensor $\frac{1}{4}(\mathbf{B}-\mathbf{B}^{-1})$ has a symmetry in its dependence upon state. It is also a second-order accurate approximation to the true strain measure of Hencky, viz., $\frac{1}{2}\ln\mathbf{B}$ (Freed 2004). Contrast this with the un-symmetric Eulerian strain measures of Signorini (1930) $\frac{1}{2}(\mathbf{B}-\mathbf{I})$ and Almansi (1911) $\frac{1}{2}(\mathbf{I}-\mathbf{B}^{-1})$ that are prevalent in the literature, both of which are first-order accurate approximations to Hencky strain. Einstein et al. (In press) and Freed et al. (In press) have found $\frac{1}{4}(\mathbf{B}-\mathbf{B}^{-1})$ to be a good strain measure for quantifying the response of the ground substance matrix in soft-tissue mechanics, where they employed this Eulerian strain measure in its Lagrangian representation which reads $\frac{1}{4}(\mathbf{I}-\mathbf{C}^{-2})$.

Whenever an invariant appears by itself in a strain-energy function, a deformation tensor ensues. Whenever the invariant sum $I+I\!I$ appears, a strain tensor is produced. Our material class is a generalization of this invariant sum, keeping in mind the constraints of Lemma 1. Let us consider a class of incompressible elastic materials whose strain-energy function is given by

$$2\varrho W = \mu\tfrac{1}{4}\big(f(\boldsymbol{p}_1;I)-f(\boldsymbol{p}_1;3)+f(\boldsymbol{p}_2;I\!I)-f(\boldsymbol{p}_2;3)\big), \tag{13}$$

where μ (>0) is the elastic shear modulus with units of stress, and $\boldsymbol{p}_i$ is a vector of parameters, which may have different values when associated with I and $I\!I$. Function f is any dimensionless function that satisfies the following constraints:

$$\begin{aligned}
\textit{physics:}\quad & f(\boldsymbol{p}_1;I)\geq 0 \;\;\&\;\; f(\boldsymbol{p}_2;I\!I)\geq 0,\\
& f'(\boldsymbol{p}_1;3)=1 \;\;\&\;\; f'(\boldsymbol{p}_2;3)=1,\\
\textit{monotonicity:}\quad & f'(\boldsymbol{p}_1;I)>0 \;\;\&\;\; f'(\boldsymbol{p}_2;I\!I)>0,\\
\textit{convexity:}\quad & f'(\boldsymbol{p}_1;I)+2If''(\boldsymbol{p}_1;I)>0 \;\;\&\\
& f'(\boldsymbol{p}_2;I\!I)+2I\!If''(\boldsymbol{p}_2;I\!I)>0,
\end{aligned} \tag{14}$$

where $f'(x):=\mathrm{d}f(x)/\mathrm{d}x$ and $f''(x):=\mathrm{d}^2f(x)/\mathrm{d}x^2$. The $f(\boldsymbol{p}_i;3)$ present in Eq. (13) are constants introduced to normalize the strain energy so that $W\geq 0$.

The definition for strain energy given in Eq. (13), in conjunction with the defining law for incompressible elasticity stated in Eq. (8), lead to an elastic constitutive equation in the Eulerian frame of

$$\mathbf{T} + \wp\,\mathbf{I} = \mu\tfrac{1}{4}\big(f'(\boldsymbol{p}_1; I)\,\mathbf{B} - f'(\boldsymbol{p}_2; I\!I)\,\mathbf{B}^{-1}\big), \quad \det\mathbf{F} = 1, \tag{15}$$

that when pulled back into the Lagrangian frame becomes

$$\mathbf{S} + \wp\,\mathbf{C}^{-1} = \mu\tfrac{1}{4}\big(f'(\boldsymbol{p}_1; I)\,\mathbf{I} - f'(\boldsymbol{p}_2; I\!I)\,\mathbf{C}^{-2}\big), \quad \det\mathbf{F} = 1, \tag{16}$$

recalling that $\varrho = \varrho_0$ because $\det\mathbf{F} = 1$. The $1/4$ is introduced here so that whenever $f' = 1$ the above equation reduces to $\mathbf{T} + \wp\,\mathbf{I} = \mu\frac{1}{4}\big(\mathbf{B} - \mathbf{B}^{-1}\big)$, wherein μ now corresponds with the classic definition of Lamé's elastic shear modulus in the domain of infinitesimal strains. This physical interpretation of μ applies to all models in our material class, because of the second line of constraints in Eq. (14). These same constraints also ensure that the right-hand side of Eq. (15) becomes $\mathbf{0}$ whenever $\mathbf{B} = \mathbf{I}$, i.e., the right-hand side is a strain measure independent of $\wp$.

Choosing a functional form for f that is in accordance with the constraints put forth in Eq. (14) will lead to an admissible constitutive equation for the modeling of elastic solids.

3.1 Human Heel Pad

Few tissues in the human body are isotropic. The calcaneal fat pad in our feet has been demonstrated via experiment to be isotropic (Miller-Young 2003). This makes the heel pad an ideal tissue to work with for the purpose of deciphering mathematical structure, and to assess capability of the AIC information theoretic in model selection through multi-model inference—a technology reviewed in App. A. Extending the structure of our model to anisotropic tissues is a topic for future work.

There are a variety of functional forms for f that one could investigate which will satisfy the constraints laid down in Eq. (14). We shall consider four models constructed from the following two basic mathematical functions:

$$\begin{aligned} f(x) &= \tfrac{1}{n+1}x^{n+1}, \qquad n > 0, \qquad x \in \{I/3, I\!I/3\}, \\ f(x) &= \tfrac{1}{n}\mathrm{e}^{nx}, \qquad\quad n > 0, \qquad x \in \{I - 3, I\!I - 3\}. \end{aligned} \tag{17}$$

Parameter μ is common to all models, while the parameter vectors $\boldsymbol{p}_i$ are equal (i.e., $\boldsymbol{p}_1 = \boldsymbol{p}_2 = \{n\}$) in two of the models, and distinct (viz., $\boldsymbol{p}_1 = \{n_1\}$ and $\boldsymbol{p}_2 = \{n_2\}$) in the other two models. The power law has a long history in tissue mechanics, dating back to Mitton (1945). More prominent in the biomechanics literature of today is the exponential law advocated by Fung (1967).

We proceed by acquiring maximum log-likelihood estimates for the unknown material parameters in each of the four candidate models, along with a suite of statistical parameters: the objective function Φ, the coefficient of variation in the data σ, the AIC information theoretic μ_{AIC} and the AIC difference Δ_i, as defined in App. A. These values have been tabulated in Table 1. Quasi-static and dynamic

$f'(x)$	μ_{qs} (kPa)	μ_{dyn} (kPa)	n_1	n_2	Φ	σ	μ_{AIC}	Δ_i
x^n	0.691	2.214	2.59	$n_2 = n_1$	5.5662	0.2395	175.0	0
x^n	0.685	2.177	5.08	1.29	5.5414	0.2390	176.7	1.7
e^{nx}	0.700	2.274	0.708	$n_2 = n_1$	5.6306	0.2409	176.1	1.1
e^{nx}	0.692	2.227	1.40	0.405	5.5722	0.2397	177.3	2.3

Table 1 Optimized parameters μ_{qs}, μ_{dyn}, n_1 and n_2 for the quasi-static and dynamic elastic responses of the human calcaneal fat pad in unconfined compression, cf. Figs. (1 & 2).

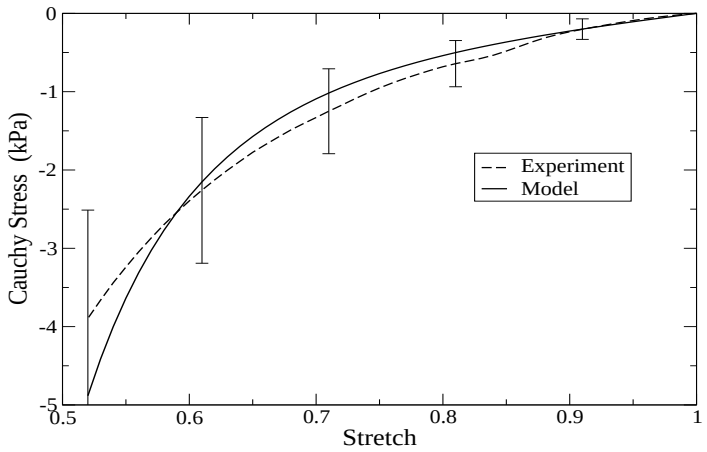

Figure 1 Quasi-static stress/stretch response to 50% deformation at $\dot{\lambda} = -10^{-3}\ \text{s}^{-1}$. Experimental mean and standard deviation data (obtained from 10 feet) are from Miller-Young (2003).

experiments were fit simultaneously—see Figs. (1 & 2). It was postulated and verified that only the shear modulus μ exhibits a rate dependence, whereas n is rate insensitive in a statistical sense, which is why there are two shear moduli reported in Table 1; they are the shear moduli belonging to these two experiments, and are not to be confused with the viscoelastic rubbery μ_∞ and glassy μ_0 shear moduli introduced in the next section.

By employing the methodology from information theory presented in App. A, an examination of the data presented in Table 1 allows one to conclude that the power-law and exponential models are both 'good' candidates for the modeling of unconfined compression in the human heel pad, with the power-law being only slightly better in this instance. The power law has an additional practical advantage over the exponential in that it is more efficient and robust in a finite element setting. For both function types, the models with $n_1 = n_2$ were found to be superior to their affiliated models where $n_1 \neq n_2$. The additional parameter present in the models where $n_1 \neq n_2$ brought no added value to these models from the perspective of information theory, allowing the simpler models where $n_1 = n_2$ to be selected. Herein lies the true worth of the AIC information theoretic: models

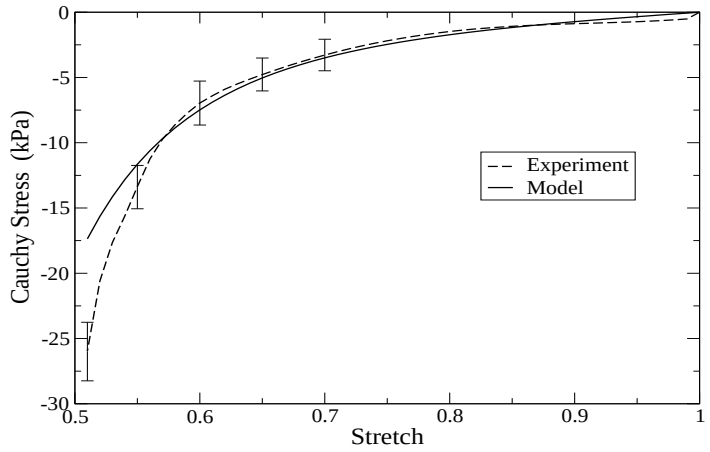

Figure 2 Dynamic stress/stretch response to 50% deformation at $\dot{\lambda} = -35\ \mathrm{s}^{-1}$. Experimental mean and standard deviation data (obtained from 7 feet) are from Miller-Young (2003).

with differing numbers of material parameters can be assessed *objectively* to determine which is best. AIC provides a metric for the Kullback-Leibler (KL) information space by which distances can be measured between various mathematical models (via the AIC differences Δ_i) whose parameters are all fit against a common data set.

Fits of the power-law model (using Eqs. 15 & 17 with $n_1 = n_2$) to the quasi-static and dynamic, experimental data sets of Miller-Young et al. (2002) can be found in Figs. 1 & 2. Although not perfect, these fits are within experimental variation up to about 45% compression ($\lambda = 0.65$). There is too much curvature in the model to correlate the quasi-static data with exacting precision. In contrast, there is not enough curvature in the model to accurately correlate the dynamic data. The model should therefore provide reasonable approximations of reality over a wide range in dynamic input. Placing 95% confidence intervals around the parameters of this fit (see Eq. A4) puts $n \in [2.30, 2.85]$, while $\mu_{\mathrm{qs}} \in [0.48, 0.90]$ kPa and $\mu_{\mathrm{dyn}} \in [1.55, 2.89]$ kPa. These are maximum-likelihood confidence intervals, which need not be symmetric about their optimum values, as is the case with least-squares confidence intervals.

4 1D FOV

In landmark papers by Caputo and Mainardi (1971a, b), the authors analytically continued the standard viscoelastic solid (Zener 1948, pg. 43)

$$\big[1 + \tau\,\mathrm{D}\big]\sigma(t) = E_\infty\big[1 + \rho\,\mathrm{D}\big]\epsilon(t), \quad \sigma_{0+} = E_\infty(\rho/\tau)\epsilon_{0+}, \tag{18}$$

by replacing its derivatives in time $\mathrm{D}f(t) := \partial f(t)/\partial t$ with the Caputo (1967) fractional derivative of order α in time (cf. Podlubny 1999, pp. 78–81)[5]

$$\mathrm{D}^{\alpha}_{\star} f(t) := \frac{1}{\Gamma(1-\alpha)} \int_{t_0}^{t} \frac{\mathrm{D}f(s)}{(t-s)^{\alpha}}\,\mathrm{d}s, \quad 0 < \alpha < 1, \;\; t > t_0, \tag{19}$$

thereby producing the constitutive equation

$$\big[1 + \tau^{\alpha}\mathrm{D}^{\alpha}_{\star}\big]\sigma(t) = E_{\infty}\big[1 + \rho^{\alpha}\mathrm{D}^{\alpha}_{\star}\big]\epsilon(t), \quad \sigma_{0+} = E_{\infty}\big(\rho/\tau\big)^{\alpha}\epsilon_{0+}, \tag{20}$$

that we call the standard FOV solid[6], which becomes the Kelvin-Zener viscoelastic solid listed in Eq. (18) whenever $\alpha = 1$. Variables σ and ε represent engineering stress and strain, respectively, with $\sigma_{0+} := \sigma(t_{0+})$ and $\epsilon_{0+} := \epsilon(t_{0+})$ specifying their initial conditions at time t_{0+} ($= t_0 + \varepsilon$, where ε is a small positive number). This 1D model has four material constants: E_{∞} (> 0) denotes the rubbery elastic modulus, α ($0 < \alpha < 1$) is the fractional order of evolution, τ (> 0) represents the characteristic relaxation time, and ρ ($> \tau$) is the characteristic retardation time, with $E_0 := (\rho/\tau)^{\alpha} E_{\infty}$ ($> E_{\infty}$) establishing the glassy elastic modulus.

Bagley and Torvik (1986) have shown that the fractional orders of differentiation for stress and strain must be equal, as originally proposed by Caputo and Mainardi (1971a), in order to ensure that this constitutive relationship is compatible with the second law of thermodynamics; specifically, they must be equal so as to guarantee non-negative dissipation during cyclic loadings.

Having unequal fractional derivatives on the two sides of the equation also introduces unbalanced shocks into the solution arising from the initial conditions, and is most evident in the Laplace domain (Bagley and Calico 1991). Shocks need to be in balance in order for the predicted stress waves to travel with finite velocity, in accordance with physical observations. Not all FOV models possess balanced shocks; for example, the popular Voigt FOV solid $\sigma(t) = E\big[1 + \rho^{\alpha}\mathrm{D}^{\alpha}_{\star}\big]\epsilon(t)$ introduced by Caputo (1967) has an unbalanced shock, and as such, predicts that stress waves will travel with infinite velocity. Material models whose stress waves are predicted to travel with infinite velocity are a known source of numeric instability in finite element codes that account for inertial effects (Belytschko et al. 2000, pg. 314).

[5] In App. B we introduce a kernel that regularizes the fractional derivative so that Eq. (19), for $0 < \alpha < 1$, takes on the form

$$\mathrm{D}^{\alpha}_{\delta} f(t) := \frac{1}{\Gamma(1-\alpha)} \int_{t_0}^{t} \frac{\mathrm{D}f(s)}{(t+\delta-s)^{\alpha}}\,\mathrm{d}s, \quad \delta > 0, \;\; \delta/(t-t_0) \ll 1,$$

where δ is a small positive number (relative to t) that effectively takes the singularity at the upper limit of integration in the Caputo derivative (19) and moves it a minute distance δ outside the interval of integration. See §4 in App. B for more details.

[6] The standard FOV fluid is defined by

$$\big[1 + \tau^{\alpha}\mathrm{D}^{\alpha}_{\star}\big]\sigma(t) = \eta^{\alpha}\mathrm{D}^{\alpha}_{\star}\epsilon(t), \quad \sigma_{0+} = (\eta/\tau)^{\alpha}\epsilon_{0+},$$

where η (> 0) is the viscosity, τ (> 0) is its characteristic relaxation time, and α ($0 < \alpha < 1$) is the fractional order of evolution.

A robust and efficient numerical algorithm capable of solving the fractional-order differential equation presented in Eq. (20) has been published by Diethelm et al. (2002, 2004, 2005).

4.1 Relaxation-Function Formulation

An analytic solution to the standard FOV solid (Eq. 20) was obtained by Caputo and Mainardi (1971a) through an application of the method of Laplace transforms. They are able to apply this technique to Eq. (20) because it is a linear differential equation, albeit of fractional order. The solution they arrived at is a special case of Boltzmann (1874) viscoelasticity, commonly written as (cf. Christensen 1971, pp. 3–9)

$$\sigma(t) = \mathcal{G}(t)\,\epsilon_{0+} + \int_{t_{0+}}^{t} \mathcal{G}(t-s)\,\frac{\partial \epsilon(s)}{\partial s}\,\mathrm{d}s. \tag{21}$$

Scaling the relaxation function $\mathcal{G}(t)$ so that it reads as

$$\mathcal{G}(t) = E_\infty + (E_0 - E_\infty)\,G(t), \tag{22}$$

with the normalized relaxation function $G(t)$ constrained so that $G_0 := G(0) = 1$ and $G_\infty := G(\infty) = 0$,[7] allows one to rewrite Eq. (21) as

$$\sigma(t) = E_\infty \epsilon(t) + (E_0 - E_\infty)\left(G(t)\,\epsilon_{0+} + \int_{t_0}^{t} G(t-s)\,\frac{\partial \epsilon(s)}{\partial s}\,\mathrm{d}s\right), \tag{23}$$

which will describe a viscoelastic solid if $E_0 > E_\infty > 0$, and a viscoelastic fluid if $E_0 > E_\infty = 0$ with the lower limit of integration then set at $t_0 = -\infty$.

For the standard FOV material models, the relaxation function has the special form

$$G(t) = E_{\alpha,1}\big(-(t/\tau)^\alpha\big), \tag{24}$$

with

$$E_{\alpha,\beta}(z) := \sum_{k=0}^{\infty} \frac{z^k}{\Gamma(\beta + \alpha k)}, \quad \alpha \in \mathbb{R}_+, \;\; \beta \in \mathbb{R}, \;\; z \in \mathbb{C}, \tag{25}$$

defining the Mittag-Leffler function (cf. Podlubny 1999, pp. 16–37), wherein $\mathbb{R}$ denotes the real line, $\mathbb{R}_+$ the positive real line, and $\mathbb{C}$ the complex plane. Equation (24) satisfies the constraints $G_0 = 1$ and $G_\infty = 0$. The Mittag-Leffler function first appeared as a relaxation function (Eq. 24) in a paper written by Gross (1947), where it was introduced in an attempt to remedy inconsistencies present in the power-law creep function. Gross did not connect the Mittag-Leffler relaxation kernel with the fractional calculus. That took place later in the papers of Caputo and Mainardi (1971a, b).

Relaxation functions described in terms of the Mittag-Leffler function, as occur in phenomenological FOV models, arise naturally from the statistical mechanics of

[7] A relaxation function with $G_0 = \infty$ is indicative of a material that propagates an impulse with infinite speed (like the Voigt FOV solid), which is not physical.

random walks made with steps taken at random intervals (Douglas 2000). Other examples of relaxation functions that have been used in soft-tissue mechanics are listed in App. B.

A straightforward summation of the series presented in Eq. (25) has regions of numeric instability whenever computations are done on machines with finite precision; therefore, equivalent expressions need to be employed in various subdomains of the function space to ensure an accurate computation of $E_{\alpha,\beta}(z)$ for all admissible values of α, β and z. Gorenflo et al. (2002) have published one such algorithm, which is more readily available in the paper of Diethelm et al. (2005).

When the fractional order α is very small, but still greater than zero, the relaxation kernel $G(t) = E_{\alpha,1}(-(t/\tau)^{\alpha})$, plotted in Fig. 3 for $\tau = 1$, drops immediately from a value of $G = 1$ at $t = 0$ to a value of $G \approx {}^1/_2$ at $t = 0^+$, from which it asymptotes algebraically, and very slowly, to zero as t goes toward infinity. Strictly speaking, the Mittag-Leffler function is not defined at $\alpha = 0$. This would be the elastic boundary where, if the Mittag-Leffler function were defined, it would exhibit a discontinuous jump so that at $\alpha = 0$ the response would be $G = {}^1/_2$ at $t = 0$ and $G = 1$ for all $t > 0$ (i.e., the Heaviside unit-step function), as there is no relaxation in the elastic limit. At the other boundary where $\alpha = 1$, relaxation is smooth and asymptotes exponentially to zero as t moves toward infinity because $E_{1,1}(-t/\tau) = \mathrm{e}^{-t/\tau}$.

For all values of α that lie within the interval $(0, 1]$, the Mittag-Leffler function provides a smooth monotone transition from a perfect elastic to a classic viscoelastic response. The function is not monotone whenever $\alpha > 1$.

4.2 Memory-Function Formulation

Infinitesimal strain is actually a two-state field that we can write as $\epsilon(t_0, t)$, where time t_0 denotes some reference state, and time t represents the deformed state. After an integration by parts, Boltzmann's viscoelastic model (23) becomes

$$\sigma(t) = E_0\epsilon(t_0, t) - (E_0 - E_\infty)\int_{t_0}^{t} M(t-s)\,\epsilon(t_0, s)\,\mathrm{d}s, \tag{26}$$

wherein $M(t-s) := \partial G(t-s)/\partial s$ defines the memory function used by Lodge (1956) in a model that he latter called the rubberlike liquid (Lodge 1964, pp. 101–104). The notion of a memory kernel was re-introduced into the biomechanics literature by Zhu et al. (1991). The terminology 'memory function' is a synonym for the 'rate-of-relaxation function'.

By utilizing additivity of infinitesimal strains (i.e., $\epsilon(t_0, t) = \epsilon(t_0, s) + \epsilon(s, t)$ for all $s \in [t_0, t]$), the above formula can be recast as

$$\sigma(t) = \big(E_\infty + (E_0 - E_\infty)\,G(t)\big)\,\epsilon(t_0, t) + (E_0 - E_\infty)\int_{t_0}^{t} M(t-s)\,\epsilon(s, t)\,\mathrm{d}s, \tag{27}$$

where now the reference state is s in the strain variable that lies under the integral sign. This is consistent with the physical notion that interval $[s, t]$ constitutes that

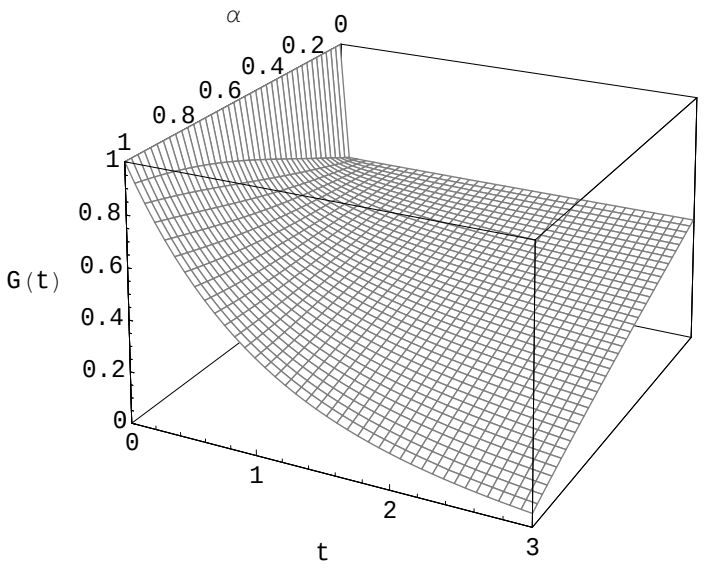

Figure 3 A 3D plot of the FOV relaxation function (i.e., Eq. 24), $G(t) = E_{\alpha,1}(-(t/\tau)^{\alpha})$, with $\tau = 1$.

part of the deformation history which the material recollects, while the preceding interval $[t_0, s)$ represents that part of the history which the material has forgotten. In this regard, Eq. (27) is preferred over Eq. (26) because it better reflects the underlying physics, even though Eq. (26) has a simpler structure and the two formulæ are equivalent. Equation (27) is also in a form amenable to the K-BKZ hypothesis.

In the testing of soft tissues, it is customary to precondition the sample prior to executing a test (Fung 1993, pp. 260–262). This has the effect of rendering down the non-integral viscoelastic contribution present in Eq. (27) to its quasi-static constituent, viz., $E_\infty \epsilon(t_0, t)$, and as such,

$$\sigma(t) = E_\infty \epsilon(t_0, t) + (E_0 - E_\infty) \int_{t_0}^{t} M(t-s)\, \epsilon(s, t)\, \mathrm{d}s \tag{28}$$

becomes the governing constitutive expression for preconditioned specimens.

The constitutive formulæ in Eqs. (26–28) are less restrictive than the constitutive formula in Eq. (23). Equations (26–28) require strain to be a C^1 function (i.e., continuous and differentiable over the deformation history); whereas, Eq. (23) requires strain to be a C^2 function (viz., continuous and twice differentiable over the deformation history).

Memory fades if $0 \leq M(t_2) < M(t_1)$ for all $t_2 > t_1 \geq t_0$, which is actually a thermodynamic requirement (Coleman and Mizel 1968). This constraint is

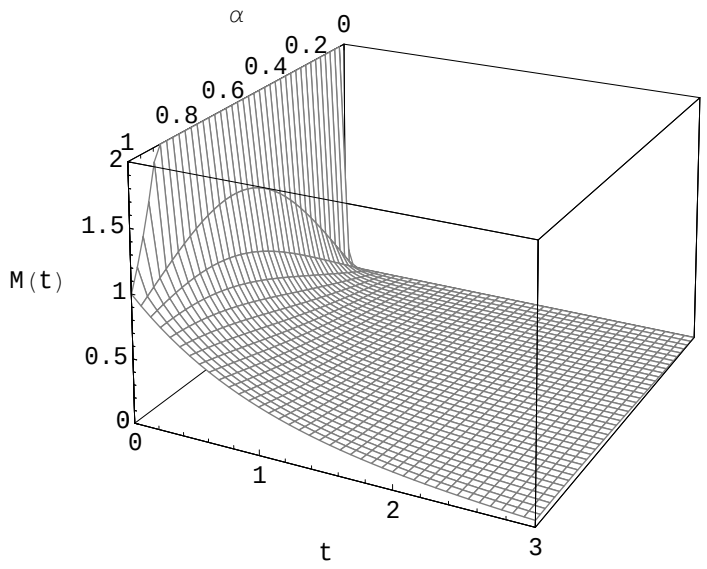

Figure 4 A 3D plot of the FOV memory function (i.e., Eq. 29), $M(t) = -E_{\alpha,0}(-(t/\tau)^{\alpha})/t$, with $\tau = 1$ where $t \in [0.001, 3]$.

satisfied by the memory function for the standard FOV solid

$$M(t) = -\frac{E_{\alpha,0}\left(-(t/\tau)^{\alpha}\right)}{t}, \tag{29}$$

where, notably, $E_{\alpha,0}(x)$ appears in the memory function, while $E_{\alpha,1}(x)$ appears in the relaxation function. The derivative $\mathrm{d}E_{\alpha,\beta}(x)/\mathrm{d}x$, which is required because of $M(t-s) = \partial G(t-s)/\partial s$, can be found in Podlubny (1999, pg. 22), for example. This kernel also appeared in the paper of Gross (1947), but it was written as $-\mathrm{d}E_{\alpha}(-(t/\tau)^{\alpha})/\mathrm{d}t$, where $E_{\alpha}(x) \equiv E_{\alpha,1}(x)$ is the one-parameter Mittag-Leffler function. Gross did not make use of the two-parameter Mittag-Leffler function $E_{\alpha,\beta}(x)$.

When the fractional order α is very small, but still greater than zero, the memory kernel $M(t) = -E_{\alpha,0}(-(t/\tau)^{\alpha})/t$, plotted in Fig. 4 for $\tau = 1$, has a response M that behaves like an impulse function, indicating that the material has a perfect knowledge of the current state. In contrast, it has virtually no recollection of even the most recent of past states. As α approaches unity, the memory function continues to maintain its perfect knowledge of the current state (i.e., M is infinite at $t = 0$, except at $\alpha = 1$, however the strength of this singularity diminishes as $\alpha \to 1$). To this complete remembrance of the current state, the function then adds an increasing recollection of past events with increasing α; albeit, this is a memory that fades away rapidly with the passage of time.

The fact that the memory function in Eq. (29) possesses a weak singularity at $M_0 := M(0)$ for all values of $\alpha \in (0, 1)$ needs to be taken into consideration when

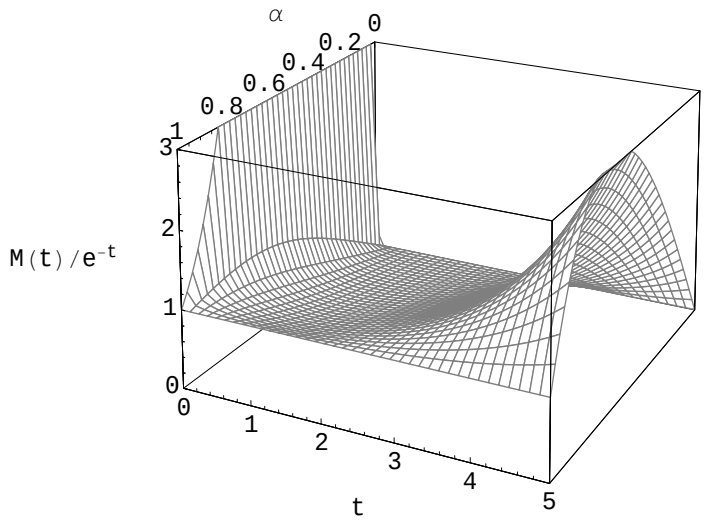

Figure 5 A 3D plot of $M(t)/\mathrm{e}^{-t} = -E_{\alpha,0}(-(t/\tau)^{\alpha})/(t\,\mathrm{e}^{-t/\tau})$ with $\tau = 1$, where $t \in [0.001, 5]$, demonstrating that the FOV memory function in Eq. (29) algebraically asymptotes to zero as $t \to \infty$ for all $\alpha \in (0, 1)$.

selecting a numerical method for solving the convolution integral that appears in Eqs. (26–28). We have constructed a unique memory-management scheme, and have coupled this with a midpoint quadrature rule with a Laplace end correction to produce an efficient (i.e., $O(N \log N)$) and accurate (viz., $O(h^5)$) numerical algorithm that solves convolution integrals like those listed in Eqs. (27 & 28), wherein the forcing function depends on both states s and t, instead of on just state t as is usually the case in convolution integrals (Diethelm and Freed in review).

A visual inspection of Figs. 3 & 4 indicates that there should be a significant numerical advantage when employing the memory function defined in Eq. (29) over its corresponding relaxation function given in Eq. (24) for the kernel of viscoelastic convolution, provided that the singularity at the upper limit of integration can be effectively and efficiently handled. Further inspection of Fig. 4 may mislead one to draw a false conclusion that the standard FOV memory function fades faster than the exponential, which is refuted in Fig. 5. For $\alpha \in (0, 1)$ and an argument t/τ that is less than about three, the FOV memory function does indeed collapse faster than exponential decay, except in a neighborhood around the origin. However, as the argument exceeds three, this trend begins to reverse and the FOV memory function starts to exhibit its true character of being algebraically asymptotic. Decay is exponential only when $\alpha = 1$.

Remark 1 The integral equation given in Eq. (27), when employing the material functions defined in Eqs. (24 & 29), is an equivalent representation of the fractional-

order differential equation stated in Eq. (20): the standard FOV *solid.* ***A practical advantage of expressing FOV as a Boltzmann integral equation with a Mittag-Leffler kernel, instead of as a fractional-order differential equation, is that a working knowledge of the fractional calculus is not required of the user in order for him/her to understand FOV to the extent that he/she can use it with confidence to solve problems of engineering interest.*** *Of course, this analog only exists if the viscoelastic response is linear for the material of interest.*

5 Viscoelasticity

We now extend this 1D formulation, and in particular Eq. (27), into a 3D theory that can be used to model soft isotropic tissues. To achieve this objective, we employ the K-BKZ hypothesis.[8] This hypothesis takes the potential structure for elasticity arising from thermostatics and analytically continues it into neighboring states of irreversibility where viscoelastic phenomena exist. The thermodynamic admissibility of this hypothesis is discussed in a separate paper by Bernstein et al. (1964).

Because most tissues are predominantly elastic, with a secondary viscoelastic attribute, and because the elastic response in these tissues is highly nonlinear, we believe that the K-BKZ hypothesis has an advantage over other approaches when it comes to developing viscoelastic models for soft tissues, the most notable alternative approach being that of internal state-variable theory (Coleman and Gurtin 1967).

Our viscoelastic model is actually constructed in App. C using convected tensor fields. The resulting formulæ are then mapped into Cartesian space-tensor formulæ by using transformation rules that are also presented in App. C. The outcomes of these transformations are the objective material models presented below: one each for the Eulerian and Lagrangian frames of reference, and a third that applies whenever strains are infinitesimal, whose derivation relies on the series expansions given in App. D.

5.1 Lagrangian Formulation

A viscoelastic material model has been derived in terms of convected tensor fields in App. C by employing the K-BKZ hypothesis. Transforming this convected model

[8] Bernstein et al. (1963) state their hypothesis thusly: "For the Coleman-Noll fluid, the stress at time t depends upon the history of the relative deformation between the configuration at time t and all configurations at times prior to t. To this idea we add the following notions: *(1)* The effect of the configuration at time $\tau < t$ on the stress at time t is equivalent to the effect of stored elastic energy with the configuration at time τ as the preferred configuration. The effect depends on $t - \tau$, the amount of time elapsed between time τ and time t. *(2)* The stress at time t is the sum (integral) of all the contributions from all $\tau < t$. ... In effect, we are taking the concept of a strain energy function associated with the theory of finite elastic deformations, which is formulated in terms of a preferred configuration, and incorporating it in a fluid theory of the Coleman-Noll type by treating all past configurations as preferred configurations."

into Cartesian space in the Lagrangian frame, using mappings that are also provided for in this appendix, leads to a decomposition in the second Piola-Kirchhoff stress $\mathbf{S}$ of the form

$$\mathbf{S} + Jp\,\mathbf{C}^{-1} = \mathbf{\Sigma}, \qquad \mathrm{tr}(\mathbf{\Sigma C}) = 0, \tag{30}$$

where the hydrostatic pressure $p = -\frac{1}{3}J^{-1}\mathrm{tr}(\mathbf{SC})$ and Lagrangian extra stress $\mathbf{\Sigma}$ are given by separate constitutive formulæ. The extra stress is deviatoric in the sense that $\mathrm{tr}(\mathbf{\Sigma C}) = 0$. Here we do not impose a constraint for incompressibility, recalling that $\frac{\varrho_0}{\varrho} = J = \det\mathbf{F} = \sqrt{\det\mathbf{C}} = \sqrt{III}$ from the conservation of mass.

Hydrostatic pressure is taken to be governed by the constitutive formula (C7)

$$p = -\kappa\,\tfrac{1}{2}\big(J - J^{-1}\big), \tag{31}$$

wherein κ is the bulk modulus. The bulk response is not considered to be viscoelastic *in vivo* in soft tissues, at least in a rate controlling sense.

The deviatoric response is taken to be governed by the constitutive equation

$$\begin{aligned}\mathbf{\Sigma} &= 2\big(\mu_\infty + (\mu_0 - \mu_\infty)\,G(t)\big)J^{-2/3}\\ &\quad\times \mathrm{DEV}\Big[\tfrac{1}{4}\big(f'(\boldsymbol{p}_1;\bar{I})\,\mathbf{I} - f'(\boldsymbol{p}_2;\bar{II})\,\bar{\mathbf{C}}^{-2}\big)\Big] + 2(\mu_0 - \mu_\infty)J^{-2/3}\\ &\quad\times\int_{t_0}^{t} M(t-s)\,\mathrm{DEV}\Big[\tfrac{1}{4}\Big(f'(\boldsymbol{p}_1;\hat{\bar{I}})\,\tilde{\bar{\mathbf{C}}}^{-1} - f'(\boldsymbol{p}_2;\hat{\bar{II}})\,\bar{\mathbf{C}}^{-1}\tilde{\bar{\mathbf{C}}}\,\bar{\mathbf{C}}^{-1}\Big)\Big]\,\mathrm{d}s,\end{aligned} \tag{32}$$

where $\mathrm{DEV}[\cdot] := (\cdot) - \frac{1}{3}\,\mathrm{tr}\,[(\cdot)\mathbf{C}]\,\mathbf{C}^{-1}$ denotes the Lagrangian deviatoric operator, while μ_∞ and μ_0 are the rubbery and glassy shear-moduli, respectively. Time t_0 is associated with a stress-free equilibrium state.

The relaxation G and memory M functions can be of whatever form one chooses (cf. App. B). They are not specified by the construction, only constrained in that $M(t-s) = \partial G(t-s)/\partial s$, $0 \le M(t_2) < M(t_1)$ for all $t_2 > t_1 \ge t_0$, $G_0 = 1$ and $G_\infty = 0$. Whenever G and M are given by Eqs. (24 & 29), respectively, Eq. (32) becomes a 3D FOV material model.

The elastic function f is left unspecified by the general construction, too. It is, however, constrained by Eq. (14) so that the overall model satisfies the K-BKZ stability criterion of Renardy (1985).

5.2 Eulerian Formulation

Mapping the convected model derived in App. C into Cartesian space in the Eulerian frame yields a decomposition in the Kirchhoff stress $\mathbf{P}(\mathbf{x};t_0,t)$ of the form

$$\mathbf{P} + Jp\,\mathbf{I} = \mathbf{\Pi}, \qquad \mathrm{tr}\,\mathbf{\Pi} = 0, \tag{33}$$

where the hydrostatic pressure $p := -\frac{1}{3}\mathrm{tr}\,\mathbf{T} = -\frac{1}{3}J^{-1}\mathrm{tr}\,\mathbf{P}$ and the Eulerian extra stress $\mathbf{\Pi}$ are governed by separate constitutive formulæ. The Kirchhoff stress $\mathbf{P}$ relates to the Cauchy stress $\mathbf{T}$ via the well-known identity $\mathbf{P} = \frac{\varrho_0}{\varrho}\mathbf{T}$ so that $\mathbf{P} = \mathbf{FSF}^{\mathrm{T}}$. The Eulerian extra stress is deviatoric in an Eulerian sense in that $\mathrm{tr}\,\mathbf{\Pi} = 0$.

The hydrostatic pressure p is still governed by Eq. (31). The Lagrangian extra stress $\mathbf{\Sigma}$ of Eq. (32) pushes forward into the Eulerian frame (i.e., $\mathbf{\Pi} = \mathbf{F}\mathbf{\Sigma}\mathbf{F}^{\mathrm{T}}$) producing

$$\mathbf{\Pi} = 2\big(\mu_\infty + (\mu_0 - \mu_\infty)\, G(t)\big)\, \mathrm{dev}\Big[\tfrac{1}{4}\big(f'(\boldsymbol{p}_1; \bar{I})\, \bar{\mathbf{B}} - f'(\boldsymbol{p}_2; \bar{II})\, \bar{\mathbf{B}}^{-1}\big)\Big] + 2(\mu_0 - \mu_\infty) \int_{t_0}^{t} M(t-s)\, \mathrm{dev}\Big[\tfrac{1}{4}\Big(f'(\boldsymbol{p}_1; \hat{\bar{I}})\, \hat{\bar{\mathbf{B}}} - f'(\boldsymbol{p}_2; \hat{\bar{II}})\, \hat{\bar{\mathbf{B}}}^{-1}\Big)\Big]\, \mathrm{d}s, \quad (34)$$

wherein $\mathrm{dev}[\cdot] := (\cdot) - \frac{1}{3}\,\mathrm{tr}(\cdot)\,\mathbf{I}$ denotes the Eulerian deviatoric operator.

The structure of the Eulerian model should be more intuitive than its Lagrangian counterpart, at least for most people.

5.3 Infinitesimal-Strain Formulation

The theoretical constructions of this paper are geared for soft biological tissues. In the case of hard biological tissues, like bone, and many engineered materials, like plastics, infinitesimal strain analysis suffices. For these materials, the previous model simplifies to an expression for engineering stress $\boldsymbol{\sigma}$ of the form

$$\boldsymbol{\sigma} + p\,\mathbf{I} = \boldsymbol{\Sigma}, \qquad \mathrm{tr}\,\boldsymbol{\Sigma} = 0, \quad (35)$$

where the hydrostatic pressure $p = -\frac{1}{3}\mathrm{tr}\,\boldsymbol{\sigma}$ is governed by

$$p = -\kappa\,\mathrm{tr}\,\boldsymbol{\epsilon}, \quad (36)$$

and the deviatoric stress $\boldsymbol{\Sigma}$ is described by

$$\boldsymbol{\Sigma} = 2\big(\mu_\infty + (\mu_0 - \mu_\infty)\, G(t)\big)\, \mathrm{dev}[\boldsymbol{\epsilon}] + 2(\mu_0 - \mu_\infty) \int_{t_0}^{t} M(t-s)\, \mathrm{dev}[\hat{\boldsymbol{\epsilon}}]\, \mathrm{d}s, \quad (37)$$

where $\boldsymbol{\epsilon} = \boldsymbol{\epsilon}(t_0, t)$ denotes engineering strain, with $\hat{\boldsymbol{\epsilon}} = \boldsymbol{\epsilon}(s, t) = \boldsymbol{\epsilon} - \tilde{\boldsymbol{\epsilon}}$ given that $\tilde{\boldsymbol{\epsilon}} = \boldsymbol{\epsilon}(t_0, s)$.

Equations (35–37) were obtained by applying the approximation formulæ listed in App. D to the above stated model in either its Lagrangian or Eulerian representation, it does not matter which.

5.4 Human Heel Pad

As an example of an isotropic viscoelastic tissue, we consider the human calcaneal fat pad; in particular, the experimental data of Miller-Young et al. (2002). The criterion of isotropy was experimentally verified, and an assumption of incompressibility has been imposed. Contrary to most soft-tissue testing, their experiments

were not preconditioned. The experiments were done in unconfined compression, and under these boundary conditions Eqs. (33 & 34) simplify to

$$\begin{aligned} T_{11} = \frac{F}{A} = \frac{\lambda F}{A_0} &= 2\big(\mu_\infty + (\mu_0 - \mu_\infty)\, G(t)\big) \\ &\times \tfrac{1}{4}\big(f'(\boldsymbol{p}_1; I)\,(\lambda^2 - \lambda^{-1}) + f'(\boldsymbol{p}_2; I\!I)\,(\lambda - \lambda^{-2})\big) + 2(\mu_0 - \mu_\infty) \\ &\times \int_{t_0}^{t} M(t-s)\, \tfrac{1}{4}\big(f'(\boldsymbol{p}_1; \hat{I})\,(\hat{\lambda}^2 - \hat{\lambda}^{-1}) + f'(\boldsymbol{p}_2; \hat{I\!I})\,(\hat{\lambda} - \hat{\lambda}^{-2})\big)\, \mathrm{d}s, \end{aligned} \tag{38}$$

where $I = \lambda^2 + 2\lambda^{-1}$ and $I\!I = 2\lambda + \lambda^{-2}$ establish the two invariants under incompressible uniaxial loading conditions, with λ being replaced by $\hat{\lambda}$ in $\hat{I}$ and $\hat{I\!I}$, which are arguments in f'. Here F is the applied force, A_0 and A are the initial and current cross-sectional areas, and $\lambda = \ell/\ell_0$ and $\hat{\lambda} = \ell/\ell_s$ are the two stretches present, with ℓ_0, ℓ_s and ℓ representing the initial, intermediate and current gage lengths of the specimen, respectively.

Because the loading history was not recorded by Miller-Young (2003) for their stress-relaxation experiment, we were forced to impose an idealized loading history. This is not desirable (Doehring et al. 2004; Gimbel et al. 2004), but it is the best one can do in this case. A deformation rate of $\dot{\lambda} = -100\ \mathrm{s}^{-1}$ was assumed, which is in the vicinity of the uppermost capabilities of modern servo-hydraulic testing equipment. This rate was applied for 0.004 s to produce a final stretch of $\lambda = 0.6$ that was then held fixed for one minute. This loading history allows the integral in Eq. (38) to be decomposed into the sum of two integrals. The first integral is over the interval of loading $t \in [t_0, t_1]$, and the second integral is over of the interval of relaxation $t \in [t_1, t_2]$. For this particular experiment, $t_0 = 0$ s, $t_1 = 0.004$ s and $t_2 = 60$ s. The advantage of breaking the integral into a sum of two integrals is that the second integral vanishes under the boundary conditions of stress relaxation, because $\hat{\lambda} = 1$ for all $s \in [t_1, t_2]$, and therefore, the forcing function (viz., strain from s to t) is zero over the entire region $[t_1, t_2]$. All arguments t in the integrand of Eq. (38) remain t whenever $t > t_1$. Only the upper limit of integration gets changed from t to t_1 in the contributing integral.

Following the method of approach used to select an elastic model, first a set of candidate viscoelastic kernels was chosen, and then the AIC information theoretic of App. A was employed to down-select the better models at describing a specified experimental data set; in this case, the stress-relaxation experiment of Miller-Young et al. (2002). The set of candidate models chosen for consideration includes: FOV, GMM, KWW, QLV and RFD, of which FOV was detailed in §4 while the latter four kernels have been described in App. B.

Because the loading data were not recorded, we assigned a value of 2.6 to the exponent n in the previously selected elastic power-law function $f'(x) = x^n$ of Eq. (17), where no distinction is made between $\boldsymbol{p}_1$ and $\boldsymbol{p}_2$, i.e., $\boldsymbol{p}_1 = \boldsymbol{p}_2 = \{n\}$. This value is in agreement with our findings from fitting the elastic data, and with the observation that it is the shear modulus μ, not the strain exponent n, that exhibits rate dependence. In all models except GMM, this leaves four parameters to be obtained via parameter estimation techniques, whose values are listed in Table 2.

Model	μ_∞ (kPa)	μ_0 (kPa)	c_1	c_2	Φ	σ	μ_{AIC}	Δ_i
FOV	0.707	4.04	0.472	0.389	0.00143	0.0114	-50.1	3.1
KWW	0.921	4.64	0.263	0.272	0.00166	0.0123	-48.4	4.8
QLV	0.965	3.41	0.0059	31.8	0.00229	0.0144	-44.9	8.3
RFD	0.711	3.79	0.366	0.069	0.00108	0.0099	-53.2	0

Table 2 Optimized shear moduli μ_∞ and μ_0, and viscoelastic kernel parameters denoted as c_1 and c_2 (see the body of the text for the mappings to their specific model parameters) for a stress relaxation of the human calcaneal fat pad, cf. Fig. (6).

Parameters in common betwixt all five models include the rubbery μ_∞ and glassy μ_0 elastic shear moduli, and the elastic stretch exponent $n = 2.6$. Except for GMM, each kernel has a relaxation/memory function pair with two material parameters that we denote as c_1 and c_2 in Table 2. These are not the notations that exist elsewhere in this paper, so here we establish their mappings and their units: For FOV, $c_1 := \alpha$ and $c_2 := \tau$ (s); for KWW, $c_1 := \beta$ and $c_2 := \tau$ (s); for QLV, $c_1 := \tau_1$ (s) and $c_2 := \tau_2$ (s); and for RFD, $c_1 := \alpha$ and $c_2 := \delta$ (s).

According to the selection criteria put forth in App. A, RFD is a 'good' model for inference, FOV lies on the boundary between 'good' and 'mediocre', while both KWW and QLV are 'mediocre' models in this regard for this material. Given this fact, RFD is the model of choice. The computational effort required to evaluate the RFD kernel is less than the computational effort required to evaluate any of the other kernels—an added bonus. The ability of RFD to correlate these data is demonstrated in Fig. 6. We reiterate that this selection process is based on the *a priori* assigned set of candidate models, and on the experimental data set chosen to fit. Different results are likely to follow given different materials, data sets and candidate models.

This outcome of RFD being the 'best' model for inference came as somewhat of a surprise to us. Our personal bias going into this exercise would have been to select the FOV kernel; this bias being based on many physically sound reasons. Biomechanicians would be apt to preselect QLV based on the biases of their backgrounds. The fact that QLV is not a good model for plantar soft tissue agrees with the recent findings of Ledoux et al. (2004). The capability of the RFD kernel, which is a generalization of the SIFS kernel proposed by Johnson et al. (1996), and the ease by which it can be computed cannot be disputed. Other than around the origin, the RFD kernel is not all that different from the Abel kernel of the fractional derivative present in the Voigt FOV model, or the Mittag-Leffler kernel present in of the Kelvin-Zener FOV model derived in §4, but it is a lot easier to work with. In effect, the RFD kernel slides the singularity at the upper limit of integration in the Voigt FOV kernel so that it lies just outside the integral by a small distance of δ. We coined the acronym RFD from the phrase *regularized fractional derivative*, because it behaves like an Abel kernel whenever $t \gg \delta$, but it does not propagate a shock wave with infinite velocity like the Voigt FOV kernel does due to the regularization imposed on the RFD kernel, viz., $G_0 = 1$ for the RFD relaxation function.

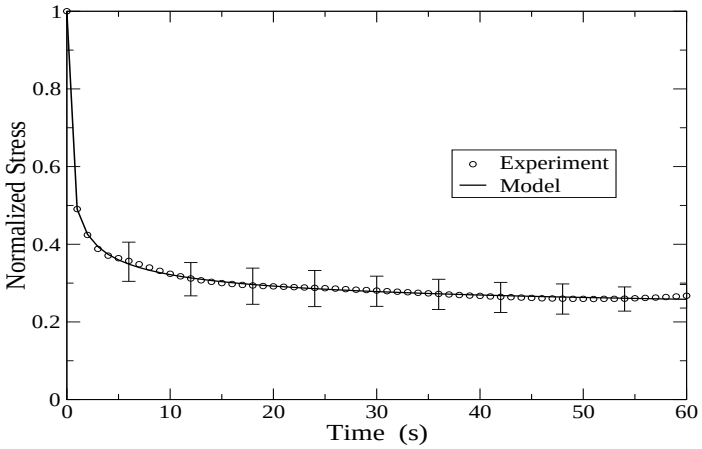

Figure 6 Stress relaxation response at 40% deformation ($\lambda = 0.6$). Experimental mean and standard deviation data (obtained from 7 feet) are from Miller-Young (2003). The mean maximum true stress was -12.7 kPa.

For the RFD model, placing 95% confidence intervals around the parameters puts: $\mu_\infty \in [0.702, 0.721]$ (kPa), $\mu_0 \in [3.75, 3.83]$ (kPa), $\alpha \in [0.363, 0.369]$ and $\delta \in [0.066, 0.072]$ (s), with n fixed at 2.6 in accordance with our elastic findings. These confidence intervals are very tight when contrasted with those obtained for the elastic model. This is because of the high precision of fit attained with the relaxation data, as contrasted with the more moderate fit achieved with the compression data. The above confidence interval for μ_∞ lies within the confidence interval for μ_{qs} obtained in §3, implying consistency between the data sets.

Conspicuously absent from the prior discussion is the GMM model, which is the *de facto* standard of the viscoelastic literature at large. The number of Maxwell chains (i.e., MM elements) considered will affect the number of material parameters present in any given GMM model. It is not uncommon in the literature to find investigators using upwards of 7 to 10 Maxwell elements in order to get a reasonable fit to a given set of experimental data. Nowhere, to our knowledge, has the AIC information theoretic been employed to answer the question: How many elements yield the 'best' Maxwell model for a given data set?

However, this very question has been asked, and answered, from the viewpoint of statistics, where the meter stick has been the minimum of some objective function. The outcome of this process is the 7 to 10 MM elements that are typically employed, with the actual number of Maxwell chains needed in any given instance being dependent upon the actual data being fit.

We now answer this same question using AIC as the meter stick. AIC is a marriage between statistics and information theory—see App. A for an overview—that enables multi-model inference. Presented in Table 3 are the maximum likelihood estimates for the parameters in three GMM models with increasing numbers of MM elements. Table 4 presents their associated AIC statistics. If one were to use the ob-

MM elements	μ_∞ (kPa)	μ_0 (kPa)	c_1	τ_1 (s)	c_2	τ_2 (s)	c_3	τ_3 (s)
$N = 1$	1.12	3.45	1	1.16	—	—	—	—
$N = 2$	0.992	3.76	$1 - c_2$	0.50	0.229	10.0	—	—
$N = 3$	0.861	3.76	$1 - c_2 - c_3$	0.45	0.181	5.05	0.119	47.6

Table 3 Optimized parameters μ_∞, μ_0, τ_1, c_2, τ_2, c_3 and τ_3 for modeling stress relaxation in the human calcaneal fat pad using the GMM kernel function.

MM elements	Φ	σ	μ_{AIC}	Δ_i
$N = 1$	0.11748	0.1033	-8.9	44.3
$N = 2$	0.00233	0.0146	-33.7	19.5
$N = 3$	0.00081	0.0086	+9.6	62.8

Table 4 AIC statistics for parameter estimates listed in Table 3.

jective function Φ as the meter stick, or equivalently, the coefficient of variation σ, then $N = 3$ MM units is obviously 'best', and it is better than any of the models presented in Table 2. Most likely, this could be improved upon still further by using even more MM elements. However, the AIC measure for multi-model inference μ_{AIC} overwhelmingly selects $N = 2$ as being the 'best' GMM model for the calcaneal fat pad. The parameters of the $N = 2$ GMM model best represent the 'information' present within the data amongst the various GMM models. Interestingly, this is the number of Maxwell chains used by Miller-Young (2003), where she reported values of $\tau_1 = 0.5$ s and $\tau_2 = 24$ s. We are in agreement on the former value but differ on the latter. Our differing values for τ_2 are likely due to the fact that we obtained our parameters from maximum log-likelihood estimates; whereas, Miller-Young obtained hers from nonlinear regression estimates. We also employed different elastic models. Furthermore, the ramp time t_1 that she imposed in her analysis was not documented.

Comparing the best GMM model against any of the previous four models via their AIC differences Δ_i ranks the best GMM as being a 'poor' material model for inference according to the criteria put forth in App. A.

6 Summary

An elastic strain-energy function has been proposed that has great potential for the field of tissue mechanics. An application of the AIC information theoretic lead to a power-law form of this free energy as being the best choice for the purpose of describing compression in the human calcaneal fat pad. The elastic material behavior associated with this free-energy function was then analytically continued into the thermodynamically irreversible domain of viscoelasticity via the K-BKZ hypothesis. Because the original K-BKZ theory was derived for fluids, and our application is for solids, we took the 1D standard FOV solid and converted it into an equivalent memory-function format. This gave us the mathematical structure of an elastic/

viscoelastic constitutive equation where strain, not strain rate, is the forcing function in the integrand, in accordance with the K-BKZ hypothesis. With this overall mathematical structure in hand, and with the 3D tensorial structure that the K-BKZ hypothesis provides (as applied to our elastic strain-energy function), a new class of viscoelastic materials was derived. A second application of the AIC information theoretic selected the RFD (regularized fractional derivative) as being the best choice for the relaxation/memory function kernels present in our material model for the purpose of describing stress relaxation in the fat pads of our feet.

We have found the AIC information theoretic to be a technology of great utility in biomechanics applications, yet it is apparently an unknown technology to this discipline. It is therefore our hope that biomechanicians will find our explanation of it to be straightforward and easy to exploit. AIC provides a means whereby we can enhance our understanding of the mathematical models that we use to describe the various behaviors that tissues exhibit.

Acknowledgements Dr. Ivan Vesely, now at Children's Hospital Los Angeles, was the PI for the project that initially supported this work. ADF thanks Dr. Peter Cavanagh for his continued support after Dr. Vesely took leave from the Cleveland Clinic. We also thank Dr. Janet Miller-Young at Mount Royal College in Calgary for supplying us with the digital data from her published experiments. We enjoyed numerous discussions/debates with Drs. Evelyn Carew, Todd Doehring and Daniel Einstein (research associates at the Cleveland Clinic at the time of this work) over applicability of the fractional calculus as a viable tool for modeling soft tissues. We thank Dr. Gena Bocharov from the Russian Academy of Sciences for making us aware of the AIC information theoretic, and instructing us in its proper use. We also thank Prof. Arkady Leonov from the University of Akron for making us aware of Renardy's lemma, and the series expansions presented in App. D. Finally, ADF thanks Prof. Ronald Bagley from the Univerisity of Texas at San Antonio for introducing him to the field of the fractional calculus and its application in viscoelasticity.

A Akaike Information Criterion

"Truth in the biological sciences and medicine is extremely complicated, and we cannot hope to find exact truth or full reality from the analysis of a finite amount of data. Thus, inference about truth must be based on a good approximating model. Likelihood and least squares methods provide a rigorous inference theory if the model structure is 'given.' However, in practical scientific problems, the model is *not* 'given.' Thus, the critical issue is, 'what is the best model to use.' This is the model selection problem." Burnham and Anderson (2002, pg. 47).

We have used theory to provide mathematical (tensorial) structure to a class of material models that contains a known (finite) set of candidates. However, theory is unable, at least in our case, to discern which candidate model is 'best', especially since our models are nonlinear. We therefore desire a methodology whose outcome will *objectively* select the best model from this set of candidate models when fit against known data prone to noise. We refrain from *subjectively* assigning the model, which is accepted practice in the biomechanics literature of today. Instead, we employ the Akaike Information Criterion (AIC)—a technology for use in model selection via multi-model inference. Other criteria also exist, see Burnham and Anderson (2002, pp. 65–70). AIC is based on the principle of parsimony: A compromise between bias-squared (simplicity - increases with decreasing numbers of model parameters) and variance (complexity - increases with increasing numbers of model parameters). AIC uses maximum log-likelihood inference to obtain 'optimum' parameter estimates for each candidate model. These estimates, in conjunction with the objective function, are then inputs into a Kullback-Leibler (KL) information-theoretic that is used to discern the 'best' model for inference, selected from the set of fitted models. The selected 'best model' need not be the 'model that fits best'.

Consider an optimization problem where:

- K is the number of candidate models,
- L is the dimension of unknown parameters $\boldsymbol{p} = [p_1, p_2, \ldots, p_L]^{\mathrm{T}}$,
- M is the dimension of state variables $\boldsymbol{y} = [y_1, y_2, \ldots, y_M]^{\mathrm{T}}$, and
- N is the number of observed variables $\boldsymbol{y}^i = [y_1^i, y_2^i, \ldots, y_M^i]^{\mathrm{T}}$, $\{t_i; y_j^i\}_{j=1:M}^{i=1:N}$, with t_i being the associated times of observation.

Consider the special case where:

1. errors between observations $\boldsymbol{y}^i$ & $\boldsymbol{y}^{i+1}$ are independent $\forall\ i \in \{1, \ldots, N-1\}$,
2. errors in observations $\boldsymbol{y}^i$ are normally distributed about the solution $\boldsymbol{y}(t_i, \widehat{\boldsymbol{p}})$, with $\widehat{\boldsymbol{p}}$ being the optimum parameters,
3. errors between y_k^i and y_ℓ^i are independent for all $k \neq \ell$ over all the i, and
4. a constant coefficient of variation exists in the observations y_j^i, which is independent of j over all the i.

If the above conditions hold, then Baker et al. (2005) have shown that the maximum log-likelihood estimate reduces to a weighted least-squares estimate whose weights are elements from the inverse of the covariance matrix of errors, which permits a

dimensionless objective function to be defined as

$$\Phi(\boldsymbol{p}) = \sum_{i=1}^{N}\sum_{j=1}^{M}\left(\frac{y_j(t_i,\boldsymbol{p}) - y_j^i}{y_j^i}\right)^2, \tag{A1}$$

implying a least-squares coefficient of variation of $\sigma = 1$; whereas, the maximum likelihood estimate for the coefficient of variation in the data is given by

$$\sigma^2 = \frac{1}{MN}\,\Phi(\widehat{\boldsymbol{p}}). \tag{A2}$$

Akaike's (cf. Burnham and Anderson 2002, pp. 60–64) measure for multi-model inference is then quantified via

$$\mu_{\text{AIC}} = MN\ln\big(\Phi(\widehat{\boldsymbol{p}})\big) + 2(L+1) + \frac{2(L+1)(L+2)}{MN-L-2}, \tag{A3}$$

wherein the $\Phi(\boldsymbol{p})$ of Eq. (A1) has been minimized to get the maximum likelihood estimates $\widehat{\boldsymbol{p}}$ for the model parameters, whose dimension L may vary from model to model; however, dimensions M and N remain fixed. The last two terms on the right-hand side of μ_{AIC} correct for model bias in the sense of KL information theory. The 'best' model for the purpose of inference is the one with the smallest or most negative μ_{AIC}.

Confidence intervals can be assigned to each parameter $\widehat{p}_\ell$ in $\widehat{\boldsymbol{p}}$. If we denote $\widetilde{\boldsymbol{p}}_\ell = [\widehat{p}_1, \widehat{p}_2, \ldots, \widehat{p}_{\ell-1}, \widetilde{p}_\ell, \widehat{p}_{\ell+1}, \ldots, \widehat{p}_L]^{\mathrm{T}}$ such that $\widetilde{p}_\ell \in [p_\ell^{\min}, p_\ell^{\max}](\chi_1^2)$, then confidence intervals are obtained via the formula (Venzon and Moolgavkar 1988)

$$MN\left|\ln\big(\Phi(\widetilde{\boldsymbol{p}}_\ell)\big) - \ln\big(\Phi(\widehat{\boldsymbol{p}})\big)\right| \le \chi_1^2, \tag{A4}$$

wherein χ_1^2 is the χ^2-distribution for 1 degree of freedom, which for the 0.95 quantile is 3.841, for example. $\Phi(\widetilde{\boldsymbol{p}}_\ell)$ varies only parameter p_ℓ from optimum $\widehat{\boldsymbol{p}}$ in a search for those values $p_\ell^{\min}$ and $p_\ell^{\max}$ that will satisfy the equality in Eq. (A4).

For a given data set, a 'best' model can be obtained by employing the straightforward methodology outlined above. But will this model be the 'best' for another data set? Maybe not. Rules have been developed that allow one to dismiss those models that are not likely to ever be 'best', while retaining a subset of 'good' models. Begin by constructing the AIC differences

$$\Delta_i = \mu_{\text{AIC}_i} - \min_{k=1}^{K}\mu_{\text{AIC}_k}. \tag{A5}$$

One then applies the following rule to infer which models are 'good', which ones are 'mediocre' and which ones are 'poor' (Burnham and Anderson 2002, pg. 70):

Δ_i	Level of Empirical Support for Model i
0–2	good model
4–7	mediocre model
> 10	poor model

It is not the absolute size of the AIC measure μ_{AIC} that matters, but rather, it is the relative value of the AIC difference Δ_i that is important. The above rule is based on the weight of evidence in favor of model i being the actual KL 'best' model for the problem at hand, given that one of the candidate models is actually this model; in other words, this rule has a solid footing in information theory.

B Other Viscoelastic Kernels

Besides the FOV kernel (a relaxation/memory function pair) presented in §4, four additional viscoelastic kernels are presented in this appendix that complete the set of candidate viscoelastic kernels used for selecting the best model for describing the dynamic behavior of the human heel pad using the AIC methodology presented in App. A. These are among the more popular relaxation/memory function pairs that appear in the viscoelastic literature.

B.1 GMM Kernel

The eminently popular Maxwell model (MM) has a generalized relaxation function of a decaying exponential

$$G(t) = \exp(-t/\tau), \tag{B1}$$

whose memory function is simply

$$M(t) = \frac{\exp(-t/\tau)}{\tau}, \tag{B2}$$

with the material constant τ (> 0) being called the characteristic time.

The generalized Maxwell model (GMM) is composed of a finite sum of N discrete MM elements such that

$$G(t) = \sum_{n=1}^{N} c_n \exp(-t/\tau_n), \quad \sum_{n=1}^{N} c_n = 1, \quad 0 < \tau_1 < \tau_2 < \cdots < \tau_N, \tag{B3}$$

whose memory function is

$$M(t) = \sum_{n=1}^{N} \frac{c_n}{\tau_n} \exp(-t/\tau_n), \tag{B4}$$

where each term in the sum can be thought of as being associated with a separate integral. It is not always possible to obtain an unique set of parameters for this model. The sum over all c_n equaling 1 enforces $G_0 = 1$, while $G_\infty = 0$ follows if $\tau_n > 0$ for all n; hence, the model obeys the principle of fading memory under these pretenses.

Without exception (to our knowledge), GMM is the viscoelastic kernel preprogrammed into commercial finite element codes that have viscoelastic material models in them. GMM is the kernel that arises from a system of first-order differential

equations describing viscoelasticity when derived from the theory of internal-state variables with N internal variables (cf. Simo and Hughes 1998, Chp. 10).

Any continuous, linear, viscoelastic spectrum can be discretized, and in doing so, can be represented with an approximating GMM kernel. Fulchiron et al. (1993) and Simhambhatla and Leonov (1993) propose using a Padé-Laplace technique to achieve this objective. Here optimum parameters to a Padé expansion of chosen order are acquired in the Laplace domain, where the problem is well posed. The results are then transformed back into the time domain for use. One usually needs about 10 Maxwell chains, i.e., 10 MM kernels or $N = 10$, in order to obtain an approximation of reasonable accuracy for a continuous spectrum whose frequency range is known over 7–10 decades.

In the thesis of Adolfsson (2003, paper 1), the Voigt FOV relaxation spectrum was discretized to obtain analytic formulæ for the Maxwell chain coefficients c_n given that $\tau_n = n\tau/N, n = 1, 2, \ldots, N$, with τ being the characteristic relaxation time from the Voigt FOV model. For a typical value for α of 0.67, he found that the normalized relaxation function predicted by 10,000 MM elements to be in about 1% error with that of the Voigt FOV relaxation function, the relaxation function obtained by using 1000 MM elements was in about 2% error, and when 100 MM elements were used it was in about 5% error.

B.2 KWW Kernel

A popular relaxation function from the viscoelastic liquids literature is the stretched exponential of Kohlrausch (1847) and Williams and Watts (1970) (KWW), which for a solid is given by

$$G(t) = \exp\left(-(t/\tau)^{\beta}\right), \tag{B5}$$

whose memory function is

$$M(t) = \frac{\beta \exp\left(-(t/\tau)^{\beta}\right)}{t^{1-\beta}\tau^{\beta}}, \tag{B6}$$

where τ (> 0) and β ($0 < \beta \leq 1$) are the material constants.

This relaxation function is normalized in the sense that $G_0 = 1$ and $G_\infty = 0$. The memory function is singular at the origin, i.e., $M_0 = \infty$ (given $0 < \beta \leq 1$), with $M(t)$ monotonically asymptoting towards $M_\infty = 0$ with increasing t. However, if β were allowed to be greater than 1, then $M_0 = M(\infty) = 0$ and the memory function would no longer be monotonic, violating the principle of fading memory. Consequently, $0 < \beta \leq 1$ in order for Eqs. (B5 & B6) to be in accordance with this physical principle.

B.3 QLV Kernel

Quasi-linear viscoelasticity (QLV) was introduced by Fung (1971), with its relaxation function not appearing until much later (Fung 1993, pg. 285). When written as a

generalized relaxation function, it becomes

$$G(t) = \frac{E_1(t/\tau_2) - E_1(t/\tau_1)}{\ln(\tau_2/\tau_1)}, \tag{B7}$$

with parameters τ_1 (> 0) and τ_2 ($> \tau_1$) designating material constants, wherein

$$E_n(x) := \int_1^\infty y^{-n}\, \mathrm{e}^{-xy}\, \mathrm{d}y \tag{B8}$$

is the exponential integral. The QLV relaxation function satisfies $G_0 = 1$ and $G_\infty = 0$. The memory function associated with this relaxation function is more user friendly, it being simply

$$M(t) = \frac{\exp(-t/\tau_2) - \exp(-t/\tau_1)}{t}. \tag{B9}$$

This has become the *de facto* standard for characterizing soft-tissue viscoelasticity in the biomechanics literature.

One needs to be careful to distinguish between the Mittag-Leffler function $E_{m,n}(x)$ (especially the one-parameter Mittag-Leffler function $E_n(x)$) and the exponential integral $E_n(x)$, all of which are their accepted notations.

The QLV relaxation function is not usually written in the above format. Specifically, E_∞ does not appear in the QLV literature; rather, a parameter c (> 0) appears that relates to the rubbery modulus via $E_\infty = E_0/[1 + c\ln(\tau_2/\tau_1)]$, where c represents the height of a box relaxation spectrum that begins at time τ_1 and ends at time τ_2. Because $M_0 = 1/\tau_1 - 1/\tau_2$ is positive, with $M(t)$ monotonically decreasing to 0 as $t \to \infty$, the QLV kernel is found to be in accordance with the principle of fading memory.

The paper of Puso and Weiss (1998) employed the GMM model, using 7 MM kernels (Eq. B3) to represent the QLV kernel (Eq. B7), so that they could approximate QLV in a finite element code in an efficient manner.

More recently, Doehring et al. (2004) applied the QLV and FOV kernels to stress relaxation and cyclic data obtained from heart-valve tissues, and found their errors in predictive capability to be similar. FOV had an advantage over QLV in their parameter estimation, as only two of QLV's three parameters were observed to be sensitive to the data. Parameter τ_2 was found to be insensitive, at least to relaxation data. This is a well-known fault of QLV. However, we did not experience this difficulty when fitting the relaxation data for the heel pad, as τ_2 was found to lie within the time interval of the relaxation experiment.

B.4 RFD Kernel

Single-integral finite-strain (SIFS) viscoelasticity (Johnson et al. 1996) employs a relaxation function of the type $G(t) = \delta/(\delta + t)$ that can be analytically continued as a power law so that the relaxation function becomes

$$G(t) = \left(\frac{\delta}{\delta + t}\right)^\alpha, \tag{B10}$$

whose affiliated memory function is just

$$M(t) = \frac{\alpha\,\delta^{\alpha}}{(\delta + t)^{\alpha+1}}, \tag{B11}$$

where α (> 0) and δ (> 0) are the material constants. Williams (1964) used this kernel to describe the relaxation behavior of solid rocket propellants and called it the modified power law.

Here $G_0 = 1$ and $G_\infty = 0$, as required, and $M_0 = \alpha/\delta$ with $M(t)$ monotonically decreasing toward $M_\infty = 0$, thereby ensuring that RFD possesses a fading memory kernel.

This kernel is not an Abel kernel, although it is similar in many respects. Specifically, Eq. (B10) is not the Voigt FOV kernel $G(t) = t^{-\alpha}/\Gamma(1-\alpha)$ associated with the fractional derivative in Eq. (19). In the Voigt FOV kernel $G_0 = \infty$ and $G_\infty = 0$, and therefore, it is singular at the upper limit of integration. Rather, Eq. (B10) is a kind of *regularized fractional derivative* (RFD) kernel whose relaxation function G is normalized so that $G_0 = 1$. This is accomplished by pushing the singularity just outside the interval of integration by a small distance δ, i.e., the singularity is moved to $t + \delta$. The Voigt FOV kernel and the RFD kernel are indistinguishable at large t. It is only when $t < \delta$ that these two kernels differ significantly. Exponent α can therefore be interpreted as a fractional order of evolution; it is the slope of the relaxation curve through the transition region between glassy and rubbery behavior. Similarities and differences between the Voigt FOV and RFD kernels have been quite thoroughly investigated by Bagley (1987).

The RFD kernel is not the only way in which a fractional derivative can be regularized. Two alternative methods have been proposed in the mathematical literature. The first one, completely different from the modified power law of RFD, is based on a discretization of the fractional derivative—see, e.g., Tuan and Gorenflo (1994a, b). The second one, described by, e.g., Rubin (1996, §11) or Gorenflo and Rubin (1994), is much closer to, but not identical with the RFD concept. Their method to tackle the singularity in the Voigt kernel mentioned above is very simple: Instead of using the full (and singular) integration range from t_0 to t in the definition of the Caputo derivative, Eq. (19), they only integrate from t_0 to $t - \delta$ with a certain (positive but small) regularization parameter δ, thus cutting off the part of the interval where the singularity appears; it still occurs at time t. Compared to our approach, their method has the charm that the correspondence between the kernel $(t - s)^{-\alpha}$ and the forcing function $f(s)$ remains unchanged; whereas, our scheme shifts one factor by an amount of δ, but does not shift the other factor simultaneously. This feature seems to be an advantage of the method of Gorenflo and Rubin. On the other hand, their cut-off strategy means that in an actual computation of the fractional derivative, which is supposed to be a functional with full but fading memory, the contribution that is associated with the most recent past (the time interval from $t - \delta$ to the current time t) is ignored completely; whereas, our method retains this information.

C Derivation of Constitutive Model

Convected tensor fields are employed in this appendix to derive our constitutive formulæ, which are then transformed into Cartesian tensor equations using well-established mapping techniques outlined in §C.2 of this appendix. This process of deriving constitutive expressions using convected tensor fields, and then mapping them into Cartesian space, ensures that the resulting Cartesian formulæ are frame invariant. The interested reader is referred to the classic paper by Oldroyd (1950) and the various textbooks of Lodge (1964, 1974, 1999) for a thorough treatment of this subject matter. Apparently, Zaremba (1903) was the first to realize that the use of convected fields automatically ensures frame indifference.

C.1 Constitutive Formulation

Consider a mass element $\boldsymbol{\xi}$ whose density is $\varrho = \varrho(\boldsymbol{\xi}; t)$, which is located by a set of components (ξ^1, ξ^2, ξ^3) in a convected coordinate system whose numeric values do *not* vary over time. Mass point $\boldsymbol{\xi}$ is put into a state of stress $\pi^{ij} = \pi^{ij}(\boldsymbol{\xi}; t)$ as the result of a change in shape $\mathrm{d}\gamma_{ij} := \gamma_{ij}(\boldsymbol{\xi}; t + \mathrm{d}t) - \gamma_{ij}(\boldsymbol{\xi}; t)$ imposed over an increment in time $\mathrm{d}t$. This deformation induces a differential change in the work done $\mathrm{d}W = \mathrm{d}W(\boldsymbol{\xi}; t, \mathrm{d}t)$ on the mass element (including an energetic contribution associated with the kinetic energy of the mass point) that is quantified by the formula (Lodge 1974, pp. 194–195)

$$\mathrm{d}W = \frac{1}{2\varrho}\,\pi^{ij}\,\mathrm{d}\gamma_{ji}, \tag{C1}$$

where repeated indices—one a subscript, the other a superscript—are summed over in the usual manner. The stress tensor $\boldsymbol{\pi}$ has contravariant components π^{ij}, the metric tensor $\boldsymbol{\gamma}$ has covariant components γ_{ij}, while the inverse metric $\boldsymbol{\gamma}^{-1}$ has contravariant components γ^{ij}. $\boldsymbol{\gamma}^{-1}$ exists because $\boldsymbol{\gamma}$ is symmetric and positive definite by definition, viz., $\mathrm{d}s^2(\boldsymbol{\xi}; t) = \mathrm{d}\xi^i(\boldsymbol{\xi})\,\gamma_{ij}(\boldsymbol{\xi}; t)\,\mathrm{d}\xi^j(\boldsymbol{\xi})$ where $\mathrm{d}s$ (> 0) is the length of infinitesimal vector $\mathrm{d}\boldsymbol{\xi}$ at particle $\boldsymbol{\xi}$ and time t.

The metric tensor $\boldsymbol{\gamma}(\boldsymbol{\xi}; t)$ of convected tensor analysis is a function of time. This characteristic is not shared by the metric tensor $\mathbf{g}(\boldsymbol{x})$ of general tensor analysis, which is independent of time (cf., e.g., with Sokolnikoff 1964).

Unlike Cartesian fields, which are evaluated in fixed, rectangular-Cartesian, coordinate systems, convected body fields are evaluated in curvilinear coordinate systems that move (i.e., convect) with the body as though the coordinate axes were drawn onto the body.

Tensors $\boldsymbol{\pi}$ and $\boldsymbol{\gamma}$ are the fundamental fields of convected tensor analysis from which constitutive equations are constructed.

From thermostatics, Eq. (C1) leads to a potential-based constitutive equation for the elastic state of stress characterized by (Lodge 1964, pp. 154–161)

$$\tfrac{\varrho_0}{\varrho}\,\pi^{ij} = \varrho_0\left(\frac{\partial W}{\partial \gamma_{ij}} + \frac{\partial W}{\partial \gamma_{ji}}\right), \quad \therefore \quad \pi^{ij} = \pi^{ji}, \tag{C2}$$

where $\varrho_0 = \varrho(\boldsymbol{\xi}\,;t_0)$. From the conservation of mass, one is lead to the expression $\frac{\varrho_0}{\varrho} = \big(\det\,(\boldsymbol{\gamma}_0^{-1}\boldsymbol{\gamma})\big)^{1/2}$ wherein the tensor contraction $\boldsymbol{\gamma}_0^{-1}\boldsymbol{\gamma}$ has mixed components $\gamma^{ik}(\boldsymbol{\xi}\,;t_0)\gamma_{kj}(\boldsymbol{\xi}\,;t)$. Symmetry in stress, a consequence of the thermostatic potential W, is also in accordance with the conservation of angular momentum.

Following the suggestion of Flory (1961), a hydrostatic/deviatoric split in the deformation field is introduced in such a way that the strain energy can be decoupled as $W = W_b + W_d$, where W_b and W_d are the bulk and deviatoric strain energies, respectively. This allows us to replace Eq. (C2) with a decomposition in the state of stress given by

$$\pi^{ij} + p\,\gamma^{ij} = \Pi^{ij}, \quad \Pi^{ij} = \Pi^{ji}, \quad \Pi^{k\ell}\gamma_{\ell k} = 0, \tag{C3}$$

wherein the hydrostatic pressure $p := -\frac{1}{3}\,\pi^{k\ell}\gamma_{\ell k}$ is governed by the constitutive equation

$$p = -\varrho_0\,\frac{\partial W_b(J)}{\partial J}, \tag{C4}$$

with $J := \big(\det(\boldsymbol{\gamma}_0^{-1}\boldsymbol{\gamma})\big)^{1/2}$ quantifying the volume of mass point $\boldsymbol{\xi}$, in a relative sense. The extra stress $\boldsymbol{\Pi}$ has contravariant components Π^{ij} that are deviatoric (i.e., $\Pi^{k\ell}\gamma_{\ell k} = 0$), and is governed by the constitutive equation

$$\tfrac{\varrho_0}{\varrho}\,\Pi^{ij} = \varrho_0 J^{-2/3}\,\mathrm{Dev}\left[\frac{\partial W_d(\boldsymbol{\gamma}_0,\overline{\boldsymbol{\gamma}})}{\partial\overline{\gamma}_{ij}} + \frac{\partial W_d(\boldsymbol{\gamma}_0,\overline{\boldsymbol{\gamma}})}{\partial\overline{\gamma}_{ji}}\right], \tag{C5}$$

with $\mathrm{Dev}[\cdot]^{ij} := (\cdot)^{ij} - \frac{1}{3}\,[(\cdot)^{k\ell}\gamma_{\ell k}]\,\gamma^{ij}$ defining the deviatoric components of a contravariant field. (We will not need the deviatoric operators for covariant and mixed tensor fields.) Tensor $\overline{\boldsymbol{\gamma}}$ has components $\overline{\gamma}_{ij} := J^{-2/3}\gamma_{ij}(\boldsymbol{\xi}\,;t)$, and is therefore isochoric because $\det(\boldsymbol{\gamma}_0^{-1}\overline{\boldsymbol{\gamma}}) = 1$. The argument $\boldsymbol{\gamma}_0$ in W_d is a constant tensor field establishing the initial shape of the mass element. It is like a built-in boundary condition.

Soft connective tissues are inherently viscoelastic. By adopting the design philosophy advocated in the K-BKZ theory of viscoelasticity (Kaye 1962; Bernstein et al. 1963), one can analytically continue the above elastic state into a viscoelastic state by employing an appropriate expression for the strain-energy gradient as the forcing function in the viscoelastic structure of Boltzmann (1874).

In soft-tissue mechanics, it is reasonable to assume that only the deviatoric response is viscoelastic. There are applications where viscoelastic compressibility can be very important (cf. Leonov 1996); however, the *in vivo* rate-controlling relaxation mechanisms of soft tissues are not known to be affiliated with volume change.

C.1.1 Bulk behavior. Soft tissues are nearly incompressible materials in that their bulk moduli are orders of magnitude greater than their shear moduli, and as such, it is reasonable to consider a convex pressure/volume model whose spherical energy is given by (Simo and Hughes 1998, pg. 361)

$$\varrho_0 W_b(J) = \kappa\,\tfrac{1}{2}\Big(\tfrac{1}{2}\big(J^2-1\big) - \ln J\Big), \tag{C6}$$

which, from Eq. (C4), yields a symmetric expression for hydrostatic pressure of the form

$$p = -\kappa\, \tfrac{1}{2}\big(J - J^{-1}\big), \tag{C7}$$

with κ being the bulk modulus. Dilatation $\frac{1}{2}\big(J - J^{-1}\big)$ is a second-order accurate approximation to the dilatation of Hencky (1928), viz., $\ln J$ (cf. Freed 2004).

Again, the viscoelastic attributes of bulk behavior are *not* considered to be rate controlling in soft-tissue mechanics. Bulk behavior is taken to be elastic, and in many cases can be assumed to be incompressible.

C.1.2 Deviatoric behavior. Using Eq. (27) as our template (i.e., the memory function formulation of 1D FOV), and using the K-BKZ hypothesis to establish mathematical structure, we postulate the existence of the following general constitutive equation for the deviatoric response of a class of viscoelastic solids

$$\begin{aligned}\tfrac{\varrho_0}{\varrho}\,\Pi^{ij} &= \big(\mu_\infty + (\mu_0 - \mu_\infty)\, G(t)\big)\\ &\quad\times \varrho_0\, J^{-2/3}\,\mathrm{Dev}\left[\frac{\partial W_d(\boldsymbol{\gamma}_0, \overline{\boldsymbol{\gamma}})}{\partial\, \overline{\gamma}_{ij}} + \frac{\partial W_d(\boldsymbol{\gamma}_0, \overline{\boldsymbol{\gamma}})}{\partial\, \overline{\gamma}_{ji}}\right] + (\mu_0 - \mu_\infty)\\ &\quad\times \int_{t_0}^{t} M(t-s)\, \varrho_s\, \widehat{J}^{-2/3}\,\mathrm{Dev}\left[\frac{\partial W_d(\boldsymbol{\gamma}_s, \widehat{\overline{\boldsymbol{\gamma}}})}{\partial\, \widehat{\overline{\gamma}}_{ij}} + \frac{\partial W_d(\boldsymbol{\gamma}_s, \widehat{\overline{\boldsymbol{\gamma}}})}{\partial\, \widehat{\overline{\gamma}}_{ji}}\right] \mathrm{d}s,\end{aligned} \tag{C8}$$

where μ_0 and μ_∞ are the glassy and rubbery shear-moduli, respectively, with $\overline{\boldsymbol{\gamma}} := J^{-2/3}\boldsymbol{\gamma}$ and $\widehat{\overline{\boldsymbol{\gamma}}} := \widehat{J}^{-2/3}\boldsymbol{\gamma}$, where $\widehat{J} := \big(\det(\boldsymbol{\gamma}_s^{-1}\boldsymbol{\gamma})\big)^{1/2}$ with $\boldsymbol{\gamma}_s$ having components $\gamma_{ij}(\boldsymbol{\xi}; s)$. Metrics $\overline{\boldsymbol{\gamma}}$ and $\widehat{\overline{\boldsymbol{\gamma}}}$ are isochoric in the sense that $\det(\boldsymbol{\gamma}_0^{-1}\overline{\boldsymbol{\gamma}}) = \det(\boldsymbol{\gamma}_s^{-1}\widehat{\overline{\boldsymbol{\gamma}}}) = 1$; furthermore, $\widehat{\overline{\boldsymbol{\gamma}}} = \overline{\boldsymbol{\gamma}}$ whenever $s = t_0$. The extra stress $\boldsymbol{\Pi}$ is completely described here by two material functions: W_d and G, because $M(t-s) = \partial G(t-s)/\partial s$ by definition.

The integral for extra stress in the above expression is in accordance with the K-BKZ hypothesis: The affect of configuration $s \le t$ on stress $\boldsymbol{\Pi}$ at time t is equivalent to the affect of elastic energy stored by the material with the configuration at time s serving as its reference state, weighted by a memory function and summed over the history of all past configurations. The integral in the theory of Kaye (1962) and Bernstein et al. (1963) goes from $-\infty$ to t; whereas, our integral goes from t_0 to t, with time t_0 being a stress-free equilibrium state. Their theory is for viscoelastic fluids; our theory is for viscoelastic solids. This is why our formulation has an elastic non-integral contribution, and why ours has an initial reference configuration associated with time t_0.

The constitutive assumption that we employ to describe the isotropic deviatoric response of biological tissue is Eq. (13). When rewritten for an arbitrary reference state $s \in [t_0, t]$, and in terms of convected fields, it becomes

$$\begin{aligned}2\varrho_0 W_d(\boldsymbol{\gamma}_0, \overline{\boldsymbol{\gamma}}) &= \mu\tfrac{1}{4}\Big(f\big(\boldsymbol{p}_1; \bar{I}\big) - f(\boldsymbol{p}_1; 3) + f\big(\boldsymbol{p}_2; \overline{II}\big) - f(\boldsymbol{p}_2; 3)\Big),\\ 2\varrho_s W_d(\boldsymbol{\gamma}_s, \widehat{\overline{\boldsymbol{\gamma}}}) &= \mu\tfrac{1}{4}\Big(f\big(\boldsymbol{p}_1; \hat{\bar{I}}\big) - f(\boldsymbol{p}_1; 3) + f\big(\boldsymbol{p}_2; \widehat{\overline{II}}\big) - f(\boldsymbol{p}_2; 3)\Big),\end{aligned} \tag{C9}$$

whose invariants are defined by

$$\begin{aligned} \bar{I} &= \mathrm{tr}\big(\boldsymbol{\gamma}_0^{-1}\bar{\boldsymbol{\gamma}}\big), \qquad & \bar{II} &= \mathrm{tr}\big(\bar{\boldsymbol{\gamma}}^{-1}\boldsymbol{\gamma}_0\big), \\ \hat{\bar{I}} &= \mathrm{tr}\big(\boldsymbol{\gamma}_s^{-1}\hat{\bar{\boldsymbol{\gamma}}}\big), \qquad & \hat{\bar{II}} &= \mathrm{tr}\big(\hat{\bar{\boldsymbol{\gamma}}}^{-1}\boldsymbol{\gamma}_s\big). \end{aligned} \tag{C10}$$

We observe in Eqs. (C9 & C10) that the assigned strain-energy function weighs the two states s and t equally, within a constant of proportionality introduced via $\boldsymbol{p}_1$ and $\boldsymbol{p}_2$. Function f is subject to the stability criteria listed in Eq. (14). After some algebra, the above definitions transform Eq. (C8) into the following constitutive model

$$\begin{aligned} \tfrac{\varrho_0}{\varrho}\,\boldsymbol{\Pi} &= 2\big(\mu_\infty + (\mu_0-\mu_\infty)\,G(t)\big) \\ &\times J^{-2/3}\,\mathrm{Dev}\big[\tfrac{1}{4}\big(f'(\boldsymbol{p}_1;\bar{I})\,\boldsymbol{\gamma}_0^{-1} - f'(\boldsymbol{p}_2;\bar{II})\,\bar{\boldsymbol{\gamma}}^{-1}\boldsymbol{\gamma}_0\bar{\boldsymbol{\gamma}}^{-1}\big)\big] + 2(\mu_0-\mu_\infty) \\ &\times \int_{t_0}^{t} M(t-s)\,\hat{J}^{-2/3}\,\mathrm{Dev}\left[\tfrac{1}{4}\left(f'(\boldsymbol{p}_1;\hat{\bar{I}})\,\boldsymbol{\gamma}_s^{-1} - f'(\boldsymbol{p}_2;\hat{\bar{II}})\,\hat{\bar{\boldsymbol{\gamma}}}^{-1}\boldsymbol{\gamma}_s\hat{\bar{\boldsymbol{\gamma}}}^{-1}\right)\right]\mathrm{d}s. \end{aligned} \tag{C11}$$

We leave the functional forms for f and G as unspecified at this time, recalling that $M(t-s) = \partial G(t-s)/\partial s$.

C.2 Field Transfer

Field transfer is a process by which convected (body) tensor fields are mapped into general (space) tensor fields or, as in our case, into Cartesian tensor fields. This has been thoroughly documented by Lodge (1964, 1972, 1974), and summarized by Freed (1995).

Because the mapping of a convected body field into a Cartesian space field is many-to-one, we use the notation $\Longrightarrow$ to denote it. The underlying mathematics of this operation are substantial and are not detailed here. They can be found in the references cited above for the reader who is interested. The field transfer operator is time dependent. Whenever a mapping is to be done at current time t, denoted as $\overset{t}{\Longrightarrow}$, the resulting Cartesian fields will be defined in the Eulerian frame. Likewise, whenever field transfer is to occur at reference time t_0, denoted as $\overset{t_0}{\Longrightarrow}$, the ensuing Cartesian fields will be defined in the Lagrangian frame.

Whenever the time dependence of the convected metric tensor $\boldsymbol{\gamma}$ coincides with the time of field transfer, the resulting Cartesian fields are the identity tensor $\mathbf{I}$; specifically,

$$\boldsymbol{\gamma} \overset{t}{\Longrightarrow} \mathbf{I}, \quad \boldsymbol{\gamma}^{-1} \overset{t}{\Longrightarrow} \mathbf{I}, \quad \boldsymbol{\gamma}_0 \overset{t_0}{\Longrightarrow} \mathbf{I}, \quad \boldsymbol{\gamma}_0^{-1} \overset{t_0}{\Longrightarrow} \mathbf{I}, \tag{C12}$$

which illustrates the many-to-one property of this mapping. The covariant, contravariant or mixed nature of a convected tensor field is lost by the field-transfer operator whenever a convected body field is mapped into a Cartesian spatial field. This property is not lost, however, whenever convected body fields are mapped into general spatial fields, which are not used in this paper.

In contrast with the mappings of Eq. (C12), deformation fields will result whenever the time dependence of the convected metric differs from the time of field transfer; in particular,

$$\boldsymbol{\gamma}_0 \overset{t}{\Longrightarrow} \mathbf{B}^{-1}, \quad \boldsymbol{\gamma}_0^{-1} \overset{t}{\Longrightarrow} \mathbf{B}, \quad \boldsymbol{\gamma} \overset{t_0}{\Longrightarrow} \mathbf{C}, \quad \boldsymbol{\gamma}^{-1} \overset{t_0}{\Longrightarrow} \mathbf{C}^{-1}, \tag{C13}$$

where $\mathbf{B}$ and $\mathbf{C}$ are the left and right (or Finger 1894 and Green 1841) deformation tensors, respectively, defined in Eq. (3).

Similarly, whenever metric fields are referenced to the dummy state of integration s, $t_0 \leq s \leq t$, for example, as they can appear in viscoelastic models, then it follows straightaway that these body metric tensors map into Cartesian space according to

$$\boldsymbol{\gamma}_s \overset{t}{\Longrightarrow} \widehat{\mathbf{B}}^{-1}, \quad \boldsymbol{\gamma}_s^{-1} \overset{t}{\Longrightarrow} \widehat{\mathbf{B}}, \quad \boldsymbol{\gamma}_s \overset{t_0}{\Longrightarrow} \widetilde{\mathbf{C}}, \quad \boldsymbol{\gamma}_s^{-1} \overset{t_0}{\Longrightarrow} \widetilde{\mathbf{C}}^{-1}, \tag{C14}$$

where $\widehat{\mathbf{B}} = \widehat{\mathbf{F}}\widehat{\mathbf{F}}^{\mathrm{T}}$ and $\widetilde{\mathbf{C}} = \widetilde{\mathbf{F}}^{\mathrm{T}}\widetilde{\mathbf{F}}$, with $\widehat{\mathbf{F}}$ and $\widetilde{\mathbf{F}}$ being defined in Eq. (2).

The convected stress tensor $\boldsymbol{\pi}$ maps into Cartesian space as $\boldsymbol{\pi} \overset{t}{\Longrightarrow} \mathbf{T}$ so that

$$\tfrac{\varrho_0}{\varrho}\,\boldsymbol{\pi} \overset{t}{\Longrightarrow} \mathbf{P} := \tfrac{\varrho_0}{\varrho}\,\mathbf{T} \quad \text{and} \quad \tfrac{\varrho_0}{\varrho}\,\boldsymbol{\pi} \overset{t_0}{\Longrightarrow} \mathbf{S} := \tfrac{\varrho_0}{\varrho}\,\mathbf{F}^{-1}\mathbf{T}\mathbf{F}^{-\mathrm{T}}, \tag{C15}$$

where $\mathbf{T}$ is the Cauchy stress, $\mathbf{P}$ is the Kirchhoff stress and $\mathbf{S}$ is the second Piola-Kirchhoff stress, all of which are symmetric.

Applying the field-transfer results given in Eqs. (C12–C15) to the constitutive formulæ listed in Eqs. (C3, C7 & C11) produces the constitutive formulæ written down in Eqs. (30–34).

D Small Strain/Rotation Relationships

A variant of one's theory is often sought that can be expressed in terms of the displacement vector $\boldsymbol{u} := \boldsymbol{x}(\boldsymbol{X}) - \boldsymbol{X}$ and its gradient $\mathbf{G} := \mathbf{F} - \mathbf{I}$, $G_{ij} = \partial u_i / \partial X_j$, through the classic tensor fields defining infinitesimal strain $\boldsymbol{\epsilon} := \frac{1}{2}\big(\mathbf{G} + \mathbf{G}^{\mathrm{T}}\big)$ and infinitesimal rotation $\boldsymbol{\omega} := \frac{1}{2}\big(\mathbf{G} - \mathbf{G}^{\mathrm{T}}\big)$, wherein the strain tensor $\boldsymbol{\epsilon}$ is symmetric (i.e., $\boldsymbol{\epsilon} = \boldsymbol{\epsilon}^{\mathrm{T}}$), while the rotation tensor $\boldsymbol{\omega}$ is skew (viz., $\boldsymbol{\omega} = -\boldsymbol{\omega}^{\mathrm{T}}$).

From these definitions, one can express the finite stretch and rotation tensors $\mathbf{U}$ and $\mathbf{R}$ (where $\mathbf{F} = \mathbf{R}\mathbf{U}$ from the polar decomposition theorem) in terms of the infinitesimal strain and rotation tensors $\boldsymbol{\epsilon}$ and $\boldsymbol{\omega}$ via the formulæ

$$\begin{aligned}
\mathbf{U} &= \exp(\boldsymbol{\epsilon}) = \mathbf{I} + \boldsymbol{\epsilon} + \tfrac{1}{2}\boldsymbol{\epsilon}^2 + \cdots, \\
\mathbf{U}^{-1} &= \exp(-\boldsymbol{\epsilon}) = \mathbf{I} - \boldsymbol{\epsilon} + \tfrac{1}{2}\boldsymbol{\epsilon}^2 - \cdots, \\
\mathbf{R} &= \exp(\boldsymbol{\omega}) = \mathbf{I} + \boldsymbol{\omega} + \tfrac{1}{2}\boldsymbol{\omega}^2 + \cdots, \\
\mathbf{R}^{\mathrm{T}} &= \exp(-\boldsymbol{\omega}) = \mathbf{I} - \boldsymbol{\omega} + \tfrac{1}{2}\boldsymbol{\omega}^2 - \cdots,
\end{aligned} \tag{D1}$$

so that the various forms of the deformation gradient become

$$\begin{aligned}
\mathbf{F} = \mathbf{R}\mathbf{U} &= \mathbf{I} + \boldsymbol{\epsilon} + \boldsymbol{\omega} + \boldsymbol{\omega}\,\boldsymbol{\epsilon} + \tfrac{1}{2}\big(\boldsymbol{\epsilon}^2 + \boldsymbol{\omega}^2\big) + \cdots\,, \\
\mathbf{F}^{\mathrm{T}} = \mathbf{U}\mathbf{R}^{\mathrm{T}} &= \mathbf{I} + \boldsymbol{\epsilon} - \boldsymbol{\omega} - \boldsymbol{\epsilon}\,\boldsymbol{\omega} + \tfrac{1}{2}\big(\boldsymbol{\epsilon}^2 + \boldsymbol{\omega}^2\big) + \cdots\,, \\
\mathbf{F}^{-1} = \mathbf{U}^{-1}\mathbf{R}^{\mathrm{T}} &= \mathbf{I} - \boldsymbol{\epsilon} - \boldsymbol{\omega} + \boldsymbol{\epsilon}\,\boldsymbol{\omega} + \tfrac{1}{2}\big(\boldsymbol{\epsilon}^2 + \boldsymbol{\omega}^2\big) - \cdots\,, \\
\mathbf{F}^{-\mathrm{T}} = \mathbf{R}\mathbf{U}^{-1} &= \mathbf{I} - \boldsymbol{\epsilon} + \boldsymbol{\omega} - \boldsymbol{\omega}\,\boldsymbol{\epsilon} + \tfrac{1}{2}\big(\boldsymbol{\epsilon}^2 + \boldsymbol{\omega}^2\big) - \cdots\,,
\end{aligned} \tag{D2}$$

which in turn produce the following expressions for the deformation tensors

$$\begin{aligned}
\mathbf{C} = \mathbf{F}^{\mathrm{T}}\mathbf{F} &= \mathbf{I} + 2\boldsymbol{\epsilon} + 2\boldsymbol{\epsilon}^2 + \cdots\,, \\
\mathbf{C}^{-1} = \mathbf{F}^{-1}\mathbf{F}^{-\mathrm{T}} &= \mathbf{I} - 2\boldsymbol{\epsilon} + 2\boldsymbol{\epsilon}^2 - \cdots\,, \\
\mathbf{B} = \mathbf{F}\mathbf{F}^{\mathrm{T}} &= \mathbf{I} + 2\boldsymbol{\epsilon} + 2(\boldsymbol{\omega}\,\boldsymbol{\epsilon} - \boldsymbol{\epsilon}\,\boldsymbol{\omega}) + 2\boldsymbol{\epsilon}^2 + \cdots\,, \\
\mathbf{B}^{-1} = \mathbf{F}^{-\mathrm{T}}\mathbf{F}^{-1} &= \mathbf{I} - 2\boldsymbol{\epsilon} - 2(\boldsymbol{\omega}\,\boldsymbol{\epsilon} - \boldsymbol{\epsilon}\,\boldsymbol{\omega}) + 2\boldsymbol{\epsilon}^2 - \cdots\,.
\end{aligned} \tag{D3}$$

Using these series expansions allows one to construct first- and second-order approximations for most finite-strain constitutive formulæ.

References

1 K. Adolfsson. *Models and Numerical Procedures for Fractional Order Viscoelasticity*. PhD thesis, Chalmers University of Technology, Göteborg, Sweden, 2003. ISBN 91-7291-382-7.

2 E. Almansi. Sulle deformazioni finite dei solidi elastici isotropi. *Rendiconti della Reale Accademia dei Lincei: Classe di scienze fisiche, matematiche e naturali*, 20:705–714, 1911.

3 R. L. Bagley. Power law and fractional calculus model of viscoelasticity. *AIAA J.*, 27:1412–1417, 1987.

4 R. L. Bagley and R. A. Calico. Fractional order state equations for the control of viscoelastically damped structures. *AIAA J. Guid. Control Dynam.*, 14:304–311, 1991.

5 R. L. Bagley and P. J. Torvik. On the fractional calculus model of viscoelastic behavior. *J. Rheol.*, 30:133–155, 1986.

6 C. T. H. Baker, G. A. Bocharov, C. A. H. Paul, and F. A. Rihan. Computational modelling with functional differential equations: Identification, selection, and sensitivity. *Appl. Numer. Math.*, 53:107–129, 2005.

7 T. Belytschko, W. K. Liu, and B. Moran. *Nonlinear Finite Elements for Continua and Structures*. John Wiley & Sons, Chichester, 2000.

8 B. Bernstein, E. A. Kearsley, and L. J. Zapas. A study of stress relaxation with finite strain. *Trans. Soc. Rheol.*, 7:391–410, 1963.

9 B. Bernstein, E. A. Kearsley, and L. J. Zapas. Thermodynamics of perfect elastic fluids. *J. Res. NBS B - Math. Phys.*, 68:103–113, 1964.

10 L. Boltzmann. Zur Theorie der elastischen Nachwirkung. *Sitzungsberichte der Kaiserlichen Akademie der Wissenschaften: Mathematisch-naturwissenschaftlichen Klasse, Wien*, 70:275–300, 1874.

11 K. P. Burnham and D. R. Anderson. *Model Selection and Multimodel Inference: A practical information-theoretic apporach*. Springer, New York, second edition, 2002.

12 M. Caputo. Linear models of dissipation whose Q is almost frequency independent–II. *Geophys. J. Roy. Astr. Soc.*, 13:529–539, 1967.

13 M. Caputo and F. Mainardi. Linear models of dissipation in anelastic solids. *Riv. Nuovo Cimento*, 1:161–198, 1971a.

14 M. Caputo and F. Mainardi. A new dissipation model based on memory mechanism. *Pure Appl. Geophys.*, 91:134–147, 1971b.

15 E. O. Carew, T. C. Doehring, J. E. Barber, A. D. Freed, and I. Vesely. Fractional-order viscoelasticity applied to heart valve tissues. In L. J. Soslowsky, T. C. Skalak, J. S. Wayne, and G. A. Livesay, editors, *Proceedings of the 2003 Summer Bioengineering Conference*, pages 721–722, Key Biscayne, FL, June 25–29 2003. ASME.

16 P. R. Cavanagh, A. A. Licata, and A. J. Rice. Exercise and pharamacological countermeasures for bone loss during long-duration space flight. *???*, In press.

17 P. R. Cavanagh, G. A. Valiant, and K. W. Misevich. Biological aspects of modeling shoe/foot interaction during running. In E. C. Frederick, editor, *Sport Shoes and Playing Surfaces*, pages 24–46, Champaign, IL, 1984. Human Kinetics Publishers.

18 Q. Chen, B. Suki, and K.-N. An. Dynamic mechanical properties of agarose gels modeled by a fractional derivative model. *ASME J. Biomech. Eng.*, 126:666–671, 2004.

19 R. M. Christensen. *Theory of Viscoelasticity: An introduction*. Academic Press, New York, 1971.

20 B. D. Coleman and M. E. Gurtin. Thermodynamics with internal state variables. *J. Chem. Phys.*, 47:597–613, 1967.

21 B. D. Coleman and V. J. Mizel. On the general theory of fading memory. *Arch. Ration. Mech. Anal.*, 29:18–31, 1968.

22 K. Diethelm, N. J. Ford, and A. D. Freed. A predictor-corrector approach for the numerical solution of fractional differential equations. *Nonlinear Dynam.*, 29:3–22, 2002.

23 K. Diethelm, N. J. Ford, and A. D. Freed. Detailed error analysis for a fractional Adams method. *Numer. Algorithms*, 36:31–52, 2004.

24 K. Diethelm, N. J. Ford, A. D. Freed, and Yu. Luchko. Algorithms for the fractional calculus: A selection of numerical methods. *Comp. Meth. Appl. Mech. Eng.*, 194:743–773, 2005.

25 K. Diethelm and A. D. Freed. An efficient algorithm for the evaluation of convolution integrals. in review.

26 T. C. Doehring, E. O. Carew, and I. Vesely. The effect of strain rate on the viscoelastic response of aortic valve tissue: A direct-fit approach. *Ann. Biomed. Eng.*, 32:223–232, 2004.

27 J. F. Douglas. Polymer science applications of path-integration, integral equations, and fractional calculus. In R. Hilfer, editor, *Applications of Fractional Calculus in Physics*, chapter 6, pages 241–330. World Scientific, Singapore, 2000.

28 D. R. Einstein, A. D. Freed, and I. Vesely. Computationally efficient constitutive model for ascending aortic wall and aortic sinus. *J. Heart Valve Dis.*, In press.

29 J. Finger. Über die allgemeinsten Beziehungen zwischen endlichen Deformationen und den zugehörigen Spannungen in aeolotropen und isotropen Substanzen. *Sitzungsberichte der Akademie der Wissenschaften, Wien*, 103:1073–1100, 1894.

30 P. J. Flory. Thermodynamic relations for high elastic materials. *Trans. Faraday Soc.*, 57:829–838, 1961.

31 A. D. Freed. Natural strain. *ASME J. Eng. Mater. Technol.*, 117:379–385, 1995.

32 A. D. Freed. Transverse-isotropic elastic and viscoelastic solids. *ASME J. Eng. Mater. Technol.*, 126:38–44, 2004.

33 A. D. Freed, D. R. Einstein, and I. Vesely. Invariant formulation for dispersed transverse isotropy in aortic heart valves: An efficient means for modeling fiber splay. *Biomech. Modeling Mechanobiol.*, In press.

34 R. Fulchiron, V. Verney, P. Cassagnau, A. Michael, P. Levoir, and J. Aubard. Deconvolution of polymer melt stress relaxation by the Padé-Laplace method. *J. Rheol.*, 37:17–34, 1993.

35 Y.-C. Fung. Elasticity of soft tissues in simple elongation. *Am. J. Physiol.*, 213:1532–1544, 1967.

36 Y.-C. Fung. Stress–strain-history relations of soft tissues in simple elongation. In Y.-C. Fung, N. Perrone, and M. Anliker, editors, *Biomechanics: Its foundations and objectives*, chapter 7, pages 181–208. Prentice-Hall, Englewood Cliffs, 1971.

37 Y.-C. Fung. *Biomechanics: Mechanical properties of living tissues*. Springer, New York, second edition, 1993.

38 J. A. Gimbel, J. J. Sarver, and L. J. Soslowsky. The effect of overshooting the target strain on estimating viscoelastic properties from stress relaxation experiments. *ASME J. Biomech. Eng.*, 126:844–848, 2004.

39 W. G. Glöckle and T. F. Nonnenmacher. A fractional calculus approach to self-similar protein dynamics. *Biophys. J.*, 68:46–53, 1995.

40 R. Gorenflo, I. Loutchko, and Yu. Luchko. Computation of the Mittag-Leffler function $E_{\alpha,\beta}(z)$ and its derivatives. *Frac. Calc. Appl. Anal.*, 5:491–518, 2002. erratum: **6** (2003), pp. 111–112.

41 R. Gorenflo and B. Rubin. Locally controllable regularization of fractional derivatives. *Inverse Probl.*, 10:881–893, 1994.

42 G. Green. On the propagation of light in crystallized media. *Trans. Cambridge Phil. Soc.*, 7: 121–140, 1841.

43 B. Gross. On creep and relaxation. *J. Appl. Phys.*, 18:212–221, 1947.

44 H. Hencky. Über die Form des Elastizitätsgesetzes bei ideal elastischen Stoffen. *Z. tech. Phys.*, 9:215–220, 1928.

45 G. A. Holzapfel. *Nonlinear Solid Mechanics: A continuum approach for engineering*. John Wiley & Sons, Chichester, 2000.

46 G. A. Johnson, G. A. Livesay, S. L-Y. Woo, and K. R. Rajagopal. A single integral finite strain viscoelastic model of ligaments and tendons. *ASME J. Biomech. Eng.*, 118:221–226, 1996.

47 A. Kaye. Non-Newtonian flow in incompressible fluids. Technical Report 134, The College of Aeronautics, Cranfield, October 1962.

48 R. Kohlrausch. Ueber das Dellmann'sche Elektrometer. *Ann. Phys. Chem.*, 72:353–405, 1847.

49 T. Lang, A. LeBlanc, H. Evans, Y. Lu, H. Genant, and A. Yu. Cortical and trabecular bone mineral loss from the spine and hip in long-duration spaceflight. *J. Bone Miner. Res.*, 19: 1006–1012, 2004.

50 W. R. Ledoux, D. F. Meaney, and H. J. Hillstrom. A quasi-linear, viscoelastic, structural model of the plantar soft tissue with frequency-sensitive damping properties. *ASME J. Biomech. Eng.*, 126:831–837, 2004.

51 A. I. Leonov. On the constitutive equations for nonisothermal bulk relaxation. *Macromolecules*, 29:8383–8386, 1996.

52 A. S. Lodge. A network theory of flow birefringence and stress in concentrated polymer solutions. *Trans. Faraday Soc.*, 52:120–130, 1956.

53 A. S. Lodge. *Elastic Liquids: An introductory vector treatment of finite-strain polymer rheology*. Academic Press, London, 1964.

54 A. S. Lodge. On the description of rheological properties of viscoelastic continua. I. body-, space-, and Cartesian-space – tensor fields. *Rheol. Acta*, 11:106–118, 1972.

55 A. S. Lodge. *Body Tensor Fields in Continuum Mechanics: With applications to polymer rheology*. Academic Press, New York, 1974.

56 A. S. Lodge. An introduction to elastomer molecular network theory. Bannatek Press, Madison, 1999. PO Box 44133, Madison, WI, (has no ISBN).

57 J. E. Miller-Young. *Factors Affecting Human Heel Pad Mechanics: A finite element study*. PhD thesis, University of Calgary, Calgary, Alberta, April 2003.

58 J. E. Miller-Young, N. A. Duncan, and G. Baroud. Material properties of the human calcaneal fat pad in compression: Experiment and theory. *J. Biomech.*, 35:1523–1531, 2002.

59 R. G. Mitton. Mechanical properties of leather fibres. *J. Soc. Leath. Trades' Ch.*, 29:169–194, 1945.

60 K. B. Oldham and J. Spanier. *The Fractional Calculus*, volume 111 of *Mathematics in Science and Engineering*. Academic Press, New York, 1974.

61 J. G. Oldroyd. On the formulation of rheological equations of state. *Proc. Roy. Soc. London*, A 200:523–541, 1950.

62 I. Podlubny. *Fractional Differential Equations: An introduction to fractional derivatives, fractional differential equations, to methods of their solution and some of their applications*, volume 198 of *Mathematics in Science and Engineering*. Academic Press, San Diego, 1999.

63 M. A. Puso and J. A. Weiss. Finite element implementation of aniostropic quasi-linear viscoelasticity using a discrete spectrum approximation. *ASME J. Biomech. Eng.*, 120:62–70, 1998.

64 M. Renardy. A local existence and uniqueness theorem for a K-BKZ-fluid. *Arch. Ration. Mech. Anal.*, 88:83–94, 1985.

65 R. S. Rivlin. Large elastic deformations of isotropic materials IV. Further developments of the general theory. *Phil. Trans. Roy. Soc. London*, A 241:379–397, 1948.

66 R. S. Rivlin and D. W. Saunders. Large elastic deformations of isotropic materials VII. Experiments on the deformation of rubber. *Phil. Trans. Roy. Soc. London*, A 243:251–288, 1951.

67 B. Rubin. *Fractional Integrals and Potentials*. Addison Wesley Longman, Harlow, 1996.

68 L. C. Shackelford, A. D. LeBlanc, T. B. Driscoll, H. J. Evans, N. J. Rianon, S. M. Smith, E. Spector, D. L. Feeback, and D. Lai. Resistance exercise as a countermeasure to disuse-induced bone loss. *J. Appl. Physiol.*, 97:119–129, 2004.

69 A. Signorini. Sulle deformazioni thermoelastiche finite. In C. W. Oseen and W. Weibull, editors, *Proceedings of the 3rd International Congress for Applied Mechanics*, volume 2, pages 80–89, Stockholm, 1930. Ab. Sveriges Litografiska Tryckerier.

70 M. Simhambhatla and A. I. Leonov. The extended Padé-Laplace method for efficient discretization of linear viscoelastic spectra. *Rheol. Acta*, 32:589–600, 1993.

71 J. C. Simo and T. J. R. Hughes. *Computational Inelasticity*, volume 7 of *Interdisciplinary Applied Mathematics*. Springer-Verlag, New York, 1998.

72 I. S. Sokolnikoff. *Tensor Analysis: Theory and applications to geometry and mechanics of continua*. John Wiley & Sons, New York, second edition, 1964.

73 B. Suki, A.-L. Barabási, and K. R. Lutchen. Lung tissue viscoelasticity: A mathematical framework and its molecular basis. *J. Appl. Physiol.*, 76:2749–2759, 1994.

74 L. R. G. Treloar. *The Physics of Rubber Elasticity*. Clarendon Press, Oxford, third edition, 1975.

75 V. K. Tuan and R. Gorenflo. The Grünwald-Letnikov difference operator and regularization of the Weyl fractional differentiation. *Z. Anal. Anwend.*, 13:537–545, 1994a.

76 V. K. Tuan and R. Gorenflo. On the regularization of fractional differentiation of arbitrary positive order. *Numer. Func. Anal. Opt.*, 15:695–711, 1994b.

77 D. J. Venzon and S. H. Moolgavkar. A method for computing profile-likelihood-based confidence intervals. *Appl. Statistician*, 37:87–94, 1988.

78 G. Williams and D. C. Watts. Non-symmetrical dielectric relaxation behaviour arising from a simple empirical decay function. *Trans. Faraday Soc.*, 66:80–85, 1970.

79 M. L. Williams. Structural analysis of viscoelastic materials. *AIAA J.*, 2:785–808, 1964.

80 H. Yuan, E. P. Ingenito, and B. Suki. Dyanmic properties of lung parenchyma: Mechanical contributions of fiber network and interstitial cells. *J. Appl. Physiol.*, 83:1420–1431, 1997.

81 H. Yuan, S. Kononov, F. A. Cavalcante, K. R. Lutchen, E. P. Ingenito, and B. Suki. Effects of collagenase and elastase on the mechanical properties of lung tissue strips. *J. Appl. Physiol.*, 89:3–14, 2000.

82 S. Zaremba. Sur une forme perfectionnée de la théorie de la relaxation. *Bull. Acad. Cracovie*, pages 594–614, Juin 1903.

83 C. Zener. *Elasticity and Anelasticity of Metals*. The University of Chicago Press, Chicago, 1948.

84 W. Zhu, W. M. Lai, and V. C. Mow. The density and strength of proteoglycan-proteoglycan interaction sites in concentrated solutions. *J. Biomech.*, 24:1007–1018, 1991.